PROCEEDINGS A

royalsocietypublishing.org/journal/rspa

Perspective

Cite this article: Ramesh R, Manipatruni S. 2021 Electric field control of magnetism. *Proc. R. Soc. A* **477**: 20200942.
https://doi.org/10.1098/rspa.2020.0942

Received: 26 November 2020
Accepted: 14 June 2021

Subject Areas:
electromagnetism, materials science

Keywords:
electric field, magnetism, microelectronics

Author for correspondence:
Ramamoorthy Ramesh
e-mail: rramesh@berkeley.edu

Electric field control of magnetism

Ramamoorthy Ramesh[1,2] and Sasikanth Manipatruni[3,4,†]

[1]Department of Physics, and [2]Department of Materials Science and Engineering, University of California, Berkeley, CA, USA
[3]Materials Sciences Division, Lawrence Berkeley National Laboratory, Berkeley, CA 94720, USA
[4]Kepler Computing, Portland, OR 97229, USA

RR, 0000-0003-0524-1332

Electric field control of magnetism is an extremely exciting area of research, from both a fundamental science and an applications perspective and has the potential to revolutionize the world of computing. To realize this will require numerous further innovations, both in the fundamental science arena as well as translating these scientific discoveries into real applications. Thus, this article will attempt to bridge the gap between condensed matter physics and the actual manifestations of the physical concepts into applications. We have attempted to paint a broad-stroke picture of the field, from the macroscale all the way down to the fundamentals of spin–orbit coupling that is a key enabler of the physics discussed. We hope it will help spur more translational research within the broad materials physics community. Needless to say, this article is written on behalf of a large number of colleagues, collaborators and researchers in the field of complex oxides as well as current and former students and postdocs who continue to pursue cutting-edge research in this field.

1. Introduction

The macro-systems perspective for this article is based on the field of information technologies, writ large. Microelectronics components and systems form an ever-increasing backbone of our society, pervading many parts of our daily life, for example, through a host of consumer electronics systems, providing sensing, actuation, communication and processing and storage of information. All of these are built upon an approximately $470B/year global market that is growing at a pace of

[†]Work done while at Intel, Components Research, Hillsboro, OR 97124.

An invited Perspective to mark the election of Ramesh Ramamoorthy to the fellowship of the Royal Society in 2020.

THE ROYAL SOCIETY PUBLISHING

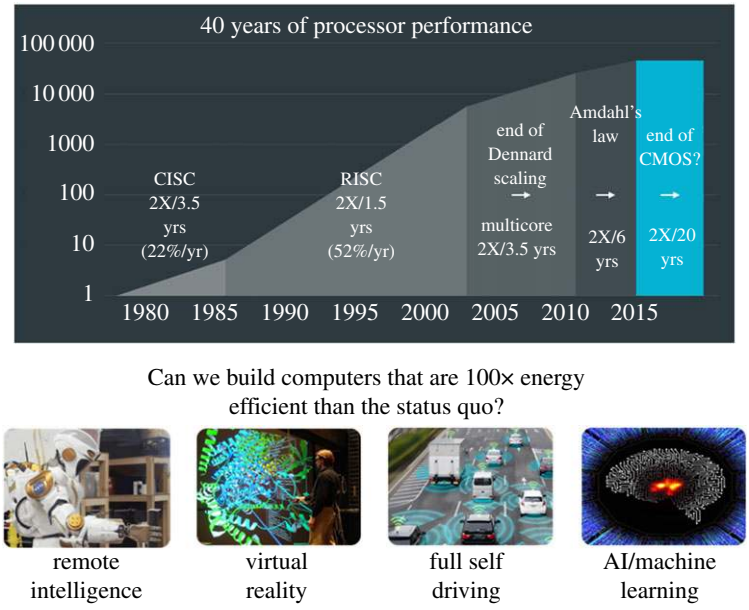

Figure 1. A schematic illustrating the emergence of the 'Internet of Things' and ML/AI as macroscale drivers for the Beyond Moore's Law R&D. Describes the leveling of the various scaling laws as a function of time, leading to the end of Moore's Law. (Online version in colour.)

10–15% annually [1,2]. Many of them likely started as materials physics research ideas, often first discussed within the confines of physics and materials conferences worldwide. A few emerging global phenomena will likely completely change this microelectronics landscape. The first among them is the 'Internet of Things' (IoT), which is the network of physical devices, transportation systems, appliances and other items embedded with electronics for sensing/actuating, computing, storage and communications functions [3], illustrated in figure 1. As an example, a modern automobile has a large number of sensing, communicating and computing components embedded and this is only going to increase; for example, the emergence of autonomous vehicles will require orders of magnitude higher levels of computing and energy efficiency of computing.

The second major phenomenon is the emergence of machine learning (ML)/artificial intelligence (AI), which is taking the technology world by storm. It uses a large amount of computing and data analytics, which, in turn, provides the system with the ability to 'learn' and do things better. Of relevance to us is the fact that microelectronic components are critical underpinnings for this field.

We can now ask the question: How do these macroscale phenomena relate to microelectronics and, more importantly, to new materials and physics underpinning them? Stated differently, what can *materials physics* do to enable this coming paradigm shift? To put this into perspective, we now need to look at the fundamental techno-economic framework that has been driving the microelectronic field for more than five decades. This is the well-known 'Moore's Law' [4], the techno-economic principle that has so far underpinned the field of microelectronics through the scaling of CMOS-based transistors (figure 2). Broadly, it states that the critical dimensions of the CMOS transistor shrink by 50% every 18–24 months. At their inception, CMOS transistors were 'macroscopic' with the critical dimension well over 1 µm and Dennard scaling provided a path to shrinking such transistors, while keeping the power density constant [4–6]. Today, this power scaling is not as easy while the critical dimensions of modern transistors are rapidly approaching sub-10 nm scales, the point at which both the fundamental science (i.e. classical electron dynamics) is no longer sufficient to adequately describe the physics of the

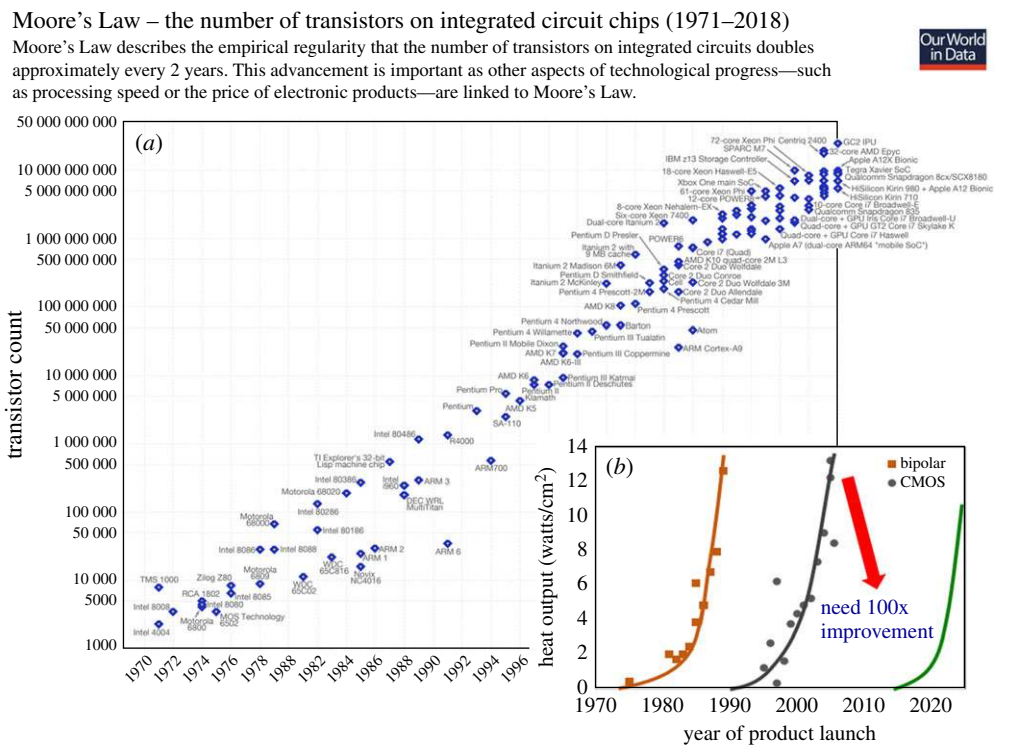

Figure 2. (*a*) Captures the evolution of semiconductor electronics, illustrating Moore's Law, which is the doubling of the number of transistors in a chip every approximately 18–24 months, versus year of implementation (source: Wikipedia); (*b*) a plot of heat output from microprocessors as a function of time for two generations of electronics, Bipolar and CMOS. Every approximately 20 years, this has led to a new paradigm of computing requiring an approximately 100× improvement in computing efficiency. The green plot is a projection of the heat output versus time for a future computing paradigm, which is at least 100× more energy efficient compared with CMOS. (Online version in colour.)

transistor and ever more complex manufacturing issues have to be addressed. Therefore, in the past 5–8 years, there has been an ever-increasing sense that something has to be done about this issue [7–11].

One can approach pathways to address this impending crisis in many ways. In some sense, this is a matter of perspective: circuit design engineers may prefer to go to specialized architectures [12] or go away from the conventional Boolean or von Neumann architecture into a Neuromorphic architecture [1]. Another pathway could be to go away from highly deterministic computing (which tolerates errors at the scale of 1×10^{-10} to 1×10^{-12} [1]) to more of a stochastic computing [13]. The third way is the one which we will be espousing, which overtly involves 'Quantum Materials', materials in which the quantum mechanical effects such as exchange interactions and spin–orbit coupling that directly lead to exotic physical phenomena (to start with magnetism, ferroelectricity, multiferroic behaviour and more recently topological behaviour arising from band topology). We get to this after a short description of another looming challenge, namely energy.

We can now introduce perhaps the single most important aspect into consideration, namely, *energy consumption* (figure 3). Of the many issues to address, energy consumption (or conversely energy efficiency of computing) has the potential to be the most impactful. The energy consumed per logic operation in today's CMOS transistor is of the order of 50–100 pJ/logic operation. If we assume that there is no change to this number in the near future, and at the same time the demand for microelectronic components in IoT and AI/ML is growing exponentially, the total energy consumption in all of microelectronics could grow to approximately 20–25% of primary energy

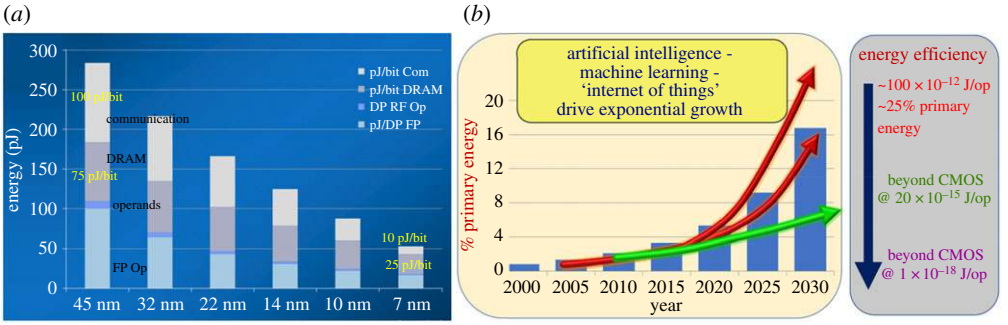

Figure 3. (*a*) Energy consumed per logic operation as a function of integration node as well as various components of the computing system (source: Shekar Borkar & Intel); (*b*) estimation of the total energy consumed in all of Microelectronics by 2030, if nothing is done to reduce the energy consumption/operation from the approximately 100 pJ/operation level, while the number of microelectronic components is growing exponentially due to the emergence of the 'Internet of Things' and AI/ML (red curves). A New Moore's Law at 20 femtojoule/operation (green curve) will enable us to keep the energy consumption at the approximately 8% level. Fundamental science is required to get to an attojoule/operation energy scale. (Online version in colour.)

by 2030 [14]. At this scale, microelectronics would become a significant part of the worldwide energy consumption and thus deserves to be addressed from the energy efficiency perspective as well. Thus, these three global phenomena form the backdrop for our discussion as we ask: *What can we do with the new materials physics?*

2. An opportunity

We begin the exploration of new materials physics by going back to the fundamentals of CMOS devices, i.e. the behaviour of an electron within the CMOS transistor that is governed by the Boltzmann distribution (figure 4*a*). A quick analysis shows that the current changes exponentially with voltage, with an ideal slope of 60 mV/decade of current [11], (figure 4*b*). This result is termed as the 'Boltzmann Tyranny' [1,10] because the Boltzmann physics is imposed as a fundamental limit on the functioning of the device; in real transistors, this voltage slope can be larger [14]. This fundamental behaviour is central to the performance of the transistor, both in terms of the minimum voltage that is required and the energy consumed in the process of operating the transistor. In recent years, there has been the realization that this Boltzmann Tyranny needs to be addressed, setting the stage for new materials and new phenomena. One proposed pathway is to use materials exhibiting a metal-to-insulator transition, such as in correlated-electron systems (figure 4*b*) [15,16]. Under ideal conditions, such a metal-to- insulator transition can be very abrupt. Another key realization [1] identifies the broad class of quantum materials as possible candidates to overcome this tyranny, mainly through the insertion of an additional, internal interaction energy into the Boltzmann distribution. A core guiding principle is that a significant opportunity exists to enable highly energy-efficient computing by exploiting correlated phenomena in materials and consequently lowering the operating voltage. Conventional CMOS has been built around non-interacting materials where the energy dissipation in such a transition is $Nk_BT\ln(2)$, where N is the number of constituent particles (e.g. spin or charge). By contrast, correlated materials (ferromagnets, ferroelectrics, multiferroics, correlated-electron systems) provide a pathway to bring down this dissipation to only $k_BT\ln(2)$. For example, this could be the exchange interaction in a ferromagnet or the dipolar interaction in ferroelectrics. In its simplest form, such an interaction can be represented by an additional term in the Hamiltonian that represents the exchange interaction energy for a magnet given by: $E_{ex} = -J \cdot S_1 \cdot S_2$, where J is the exchange integral and S_1 and S_2 are the two

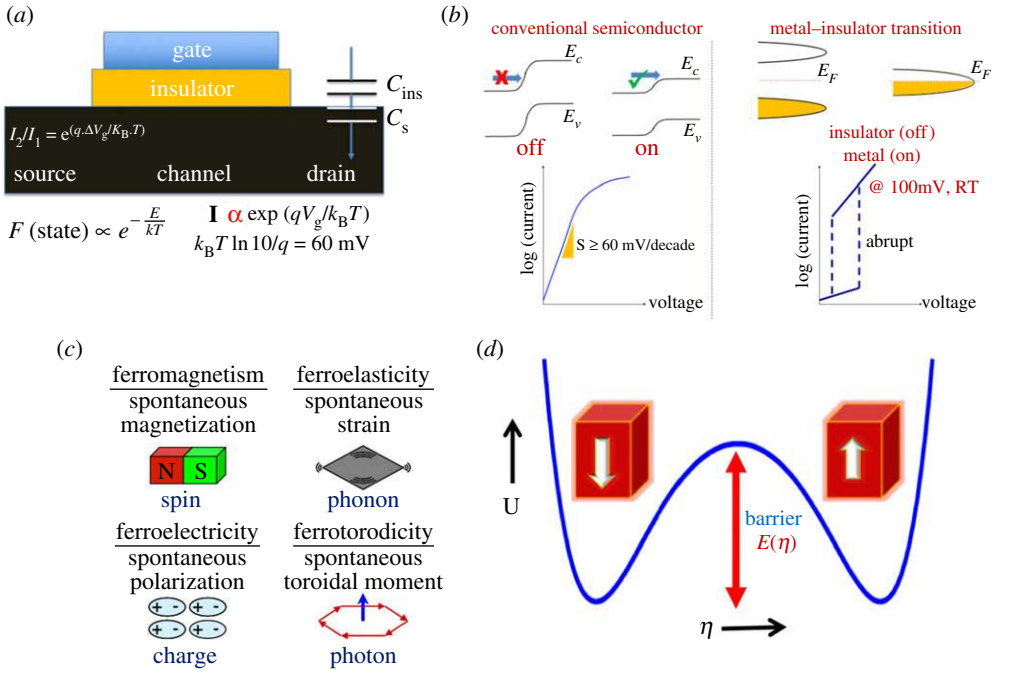

Figure 4. (*a*) Schematically describes the Boltzmann distribution function for electrons in the CMOS channel, leading to the 60 mV/decade of current as the limit, which is known as the 'Boltzmann Tyranny', shown in (*b*) which also shows a possible manifestation of metal–insulator transition as the base for the next generation of logic; (*c*) the various fundamental order parameters in condensed matter systems and the external carrier of the order parameter; (*d*) schematically describes the ratio of the energy required to switch a ferroelectric element compared with the barrier height. (Online version in colour.)

neighbouring spins (or the corresponding dipolar energy in the case of a ferroelectric). Depending on the sign of J, S_1 and S_2 are either parallel (ferromagnet) or antiparallel (antiferromagnet) [17]. This term then becomes the key component within the Boltzmann distribution and it modifies the energy landscape. That is, the exchange energy (or the dipolar energy in a ferroelectric) makes the spins (or the dipoles) align collectively *without the need* for an external source of energy (such as an applied field). Therefore, orders of magnitude improvement in energy efficiency are possible by exploiting correlations (electronic charge/spin and dipolar). Thus, if one could use a spontaneous magnetic/dipole moment as the primary order parameter rather than electronic charge in a CMOS device, one could take advantage of such internal collective order to reduce the energy consumption. Indeed, this is the premise behind two recent research articles [1,10], where the rudiments of a possible magnetoelectric spin–orbit (MESO) coupled memory-logic device are discussed. While many parts of this device require further research innovation, one aspect that we will focus on pertains to electric field control of magnetism.

3. Electric field control of magnetism: the key role of energy consumption

We can begin this discussion with a question: Why would one use an electric field to control magnetism, when it would rather be straightforward to use a magnetic field instead? The answer is energy. In fact, one can potentially reduce the energy consumption by a few orders of magnitude through the use of electric fields as opposed to magnetic fields. To illustrate this, we explore two possible scenarios. The first describes how a moving electron can create a spin torque, of interest in spin transfer torque (STT)-based memory devices [18]. The key is that each electron carries a moment of 1 μ_B and therefore generating a large enough spin torque to switch the magnetization

requires a large number of electrons (i.e. a large current), which, in turn, requires an appropriate current source (e.g. a battery). For a nominal device lateral dimension (e.g. 10×10 nm), one can estimate the energy consumed ($E_{STT} = I_{STT} \cdot V_d \cdot t_{STT}$) in this process, and it is of the order of a few fJ (10^{-15} J, figure 5*a*). Recent developments in using spin–orbit torques may very well supersede these, but that would require efficiencies orders higher than what is currently possible; thus requiring more fundamental physics innovations [1,10]. One can contrast this to a capacitive device, with an electric field modulating the charge, where for a similar 10×10 nm device with a dielectric constant of approximately 100 (which is reasonable for ferroelectrics), one can generate relatively large fields of the order of 10 kV cm^{-1} consuming just about an aJ of energy (10^{-18} J, (figure 5*b*), for a voltage of 100 mV ($E = 1/2\,CV^2$). One could ask the converse question, namely, why not use a ferroelectric and thus use a spontaneous dipole as the order parameter? Indeed, this could be possible and attempts are underway to explore the possibility of using a ferroelectric as the medium for both logic and memory. The advantage with using the spin as the primary order parameter is that one can use the huge knowledge base of spintronics and indeed carry out logic operations with spins [10].

In order to calibrate these observations, let us now look at the energy scales in magnetic and electric fields. As an extreme exemplar, we look at the manganites, which exhibit both colossal magnetoresistance as well as colossal electroresistance [15,19], as illustrated in figure 5*c*. The colossal magnetoresistance is obtained with a magnetic field of 6 T, while the corresponding colossal electroresistance is achieved with an electric field of 400 kV cm^{-1}. We can now ask the question: What is required to create both these fields? Focusing first on the magnetic field (figure 5*d*, top panel), shows that if a magnetic field of 6 T is to be created at a distance of 1 µm from a wire carrying an electrical current (the classical way to create a magnetic field using Ampere's Law), that current would be of the order of approximately 30 A. While this is a relatively small energy scale from a physics perspective, from an engineering or energy perspective, this current is significant. It is also noteworthy that this magnetic field is the same (i.e. 6 T) whether the sample is a millimetre-sized crystal or a 100 nm thick film. By contrast, if we look at the electric field-driven colossal electroresistance at a field of 400 kV cm^{-1}: this corresponds to an applied voltage of 4 V across a 100 nm thick film; if it becomes a 1 mm size crystal, the voltage required is 40 000 V. A second, key learning from this is that if one is dealing with thin films and nanostructures, where the physical length scales are small, electric fields (and thus voltages) are more useful from a technological perspective. Thus, this figure is perhaps one of the key learnings (at least from our perspective): namely, voltage (i.e. electric field) is a much more energy-efficient pathway to manipulate states, if the physics of that state allows one to do so. For the same reason, one has to be aware of the fundamental differences between the various symmetries in solids (in terms of whether they break time-reversal or spatial inversion symmetry). Finally, and perhaps more importantly, regarding this article and the work on electric field control of magnetism, it is important to ensure that physical phenomena exist that will enable us to manipulate the magnetic state with an electric field. The existence of magnetoelectricity and coupled multiferroic order does provide us with such a pathway.

With this as background, let us now explore the physics of electric field control of magnetism with a focus on multiferroic and magnetoelectric materials. Needless to say, the pace and breadth of the work in this field means that it will be impossible to cover all the developments. Furthermore, this article is also somewhat of a personal perspective of the field; therefore, the reader is requested to look at a number of excellent recent reviews [20,21] on this subject for in-depth information on other aspects of such approaches. Particularly, Song *et al*. [20] outlines several possible pathways for manipulation of magnetism (carrier modulation, strain effect, exchange coupling, orbital reconstruction and electrochemical effects), all of which play some complementary role in some of the discussion on magnetoelectric coupling in La-substituted $BiFeO_3$ that follows. Therefore, instead of reproducing that in our review, here we review progress in the fundamental understanding and design of new multiferroic materials, advances in characterization and modelling tools to describe them, and explore devices and applications. We identify the key open questions in the field where targeted

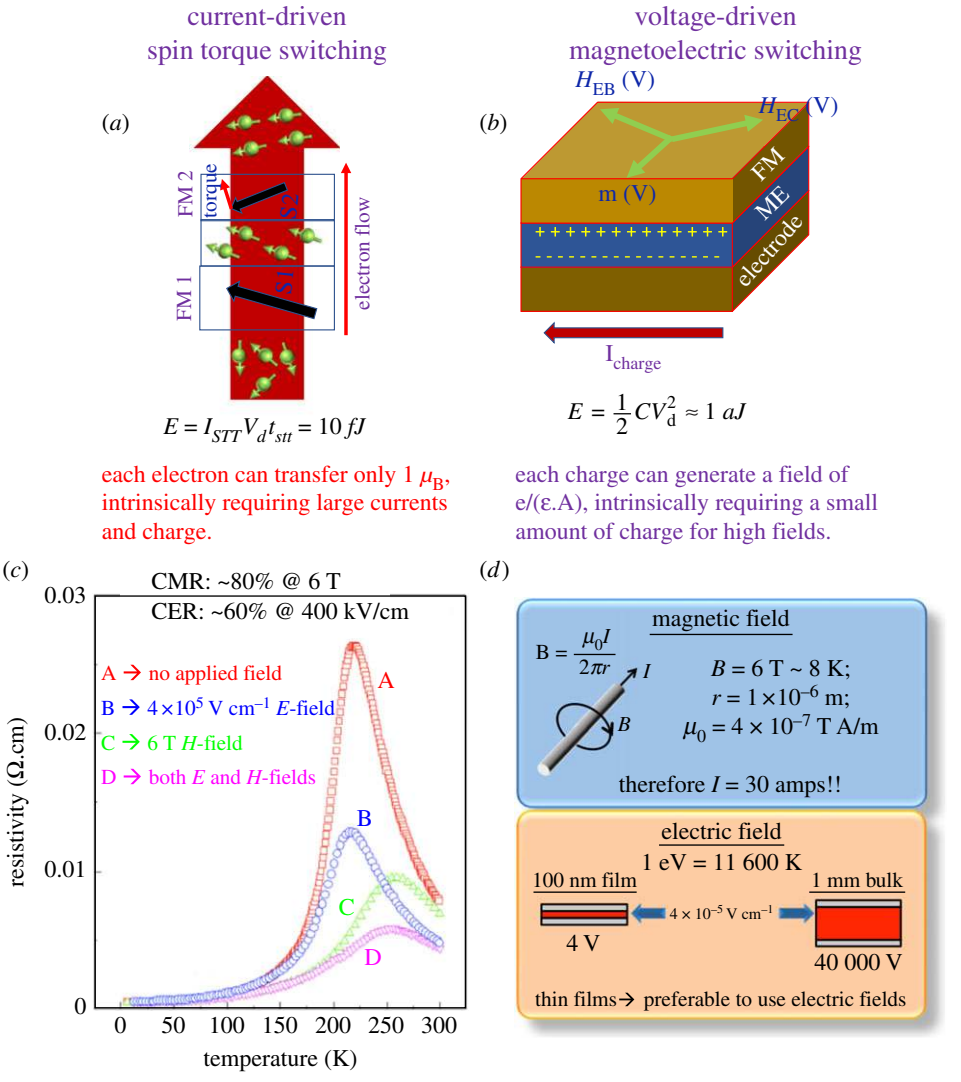

Figure 5. A set of schematics illustrating the energy consumption for nominal devices. (*a*) On the left is a current-driven spin torque switching device and (*b*) a voltage-driven magnetoelectric switch in which FM is the ferromagnet, ME is the magnetoelectric, H_{EB}(V) is the voltage-manipulated exchange bias, H_{EC}(V) is the voltage-manipulated exchange coupling and m(V) is the voltage-manipulated magnetic state in the ferromagnet; (*c*) presents the original data for the colossal magnetoresistance effect of approximately 80% at 6 T and an approximately 60% colossal electroresistance effect at an electric field of 400 kV cm^{-1}; (*d*) (top) a simple calculation of the current required to create a magnetic field of 6 T at a distance of 1 µm from the centre of the current-carrying wire while the bottom shows the calculation of the voltage required to create the 400 kV cm^{-1} electric field. This voltage scales with the dimensions of the object, while the magnetic field does not scale with the dimensions of the object. (Online version in colour.)

research activities could have maximum impact in transitioning scientific discoveries into real applications.

4. Multiferroics and magnetoelectrics

Multiferroics exhibit more than one primary ferroic ordering (i.e. ferromagnetism, ferroelectricity, ferroelasticity or ferrotoroidicity) in the same phase [22]. The terminology is usually extended

to include other types of order such as antiferromagnetism (AFM) as well as composites of individual ferroics and is most often used to refer specifically to magnetoelectric [23] materials combining ferroelectric and magnetic behaviour in a single material. The coexistence of ferroic orders can lead to coupling between them, so that one ferroic property can be manipulated with the conjugate field of the other [24,25]. A good example of a multiferroic is the case of ferromagnetic shape memory alloys (FSMA), which exhibit ferromagnetism along with a spontaneous strain [26]. Similarly, piezoelectrics combine a spontaneous strain along with a spontaneous polarization. There are numerous examples of both FSMA and piezoelectrics. By contrast, the coexistence of spin and charge order (particularly ferromagnetism and ferroelectricity) is challenging, because ferroelectricity requires an insulator while typical ferromagnets require electronic exchange interactions [27]. Many insulating magnets are either antiferromagnets or ferrimagnets (driven by super-exchange interaction). This requires understanding the electronic structure at the most fundamental level, new materials chemistries to implement them, the development of new tools to compute and characterize the novel properties associated with the coupled behaviours in parallel with new approaches to synthesize such materials with atomic-scale precision. When this is successful, it presents possible routes to entirely new device architectures, as exemplified by the MESO [9] device. The field of multiferroics is now vast, we would direct the reader to other recent reviews with different emphases [28–32].

5. Pathways to design multiferroic and magnetoelectric materials

There are now many established routes to circumvent the 'contra-indication' between ferroelectricity (typically associated with ionic species with empty *d*-orbitals) and magnetism (typically associated with partially filled *d*-orbitals) [24]. Such a 'bottom-up' design can be described by a 'multiferroic-tree' in figure 6 [21]. Although there are several known multiferroics, there is still a dearth of technologically viable multiferroics, i.e. those that can be manipulated at room temperature and exhibit strong coupling between the spin and charge degrees of freedom. Thus, there should be no doubt that a more diverse palette of new materials with robust room temperature coupling of magnetism and ferroelectricity is still urgently needed and indeed should be the focus of interdisciplinary research. Table 1 provides a summary of the top five physical principles that have led to the discovery of several multiferroics. Of these, the two most studied are multiferroics, in which the polar order comes from one of the crystal sites and the magnetic order is built into the other chemical site, as is the case, for example, in $BiFeO_3$ and $BiMnO_3$. The second type, which has received considerable interest from the physics community, is based on a polar order emerging as a consequence of a magnetic transition as, for example, in the manganites [33]. An emerging third pathway is *via* the power of heteroepitaxy and superlattice design [34]. In this regard, although there were numerous attempts in the past to synthesize complex crystal symmetries to induce multiferroic behaviour, this has not been extensively revisited in recent years. There appears to be a significant opportunity to 'design' multiferroic behaviour by selecting magnetic materials with low symmetry and then induce inversion symmetry breaking through heteroepitaxy. We will use these as examples to explore both the fundamental materials physics of coupling as well as the potential for future applications. We will revisit this issue of new materials discovery in the last segment of this article.

Of the known multiferroics, bismuth ferrite, $BiFeO_3$(BFO), remains arguably the most important, and certainly the most widely studied, with more than 6000 papers published over the last decade. The establishment of its large (approx. $90\,\mu C\,cm^{-2}$) ferroelectric polarization, combined with magnetic ordering persisting well above room temperature [35], has spawned an intense research effort that continues to unveil fascinating new physics and potential new applications [36].

$BiFeO_3$ formally belongs to the perovskite family of oxides, albeit highly rhombohedrally distorted from the cubic prototypical structure, in which the spontaneous polarization points along the eight equivalent ⟨111⟩ directions (figure 7). While there was considerable debate in the

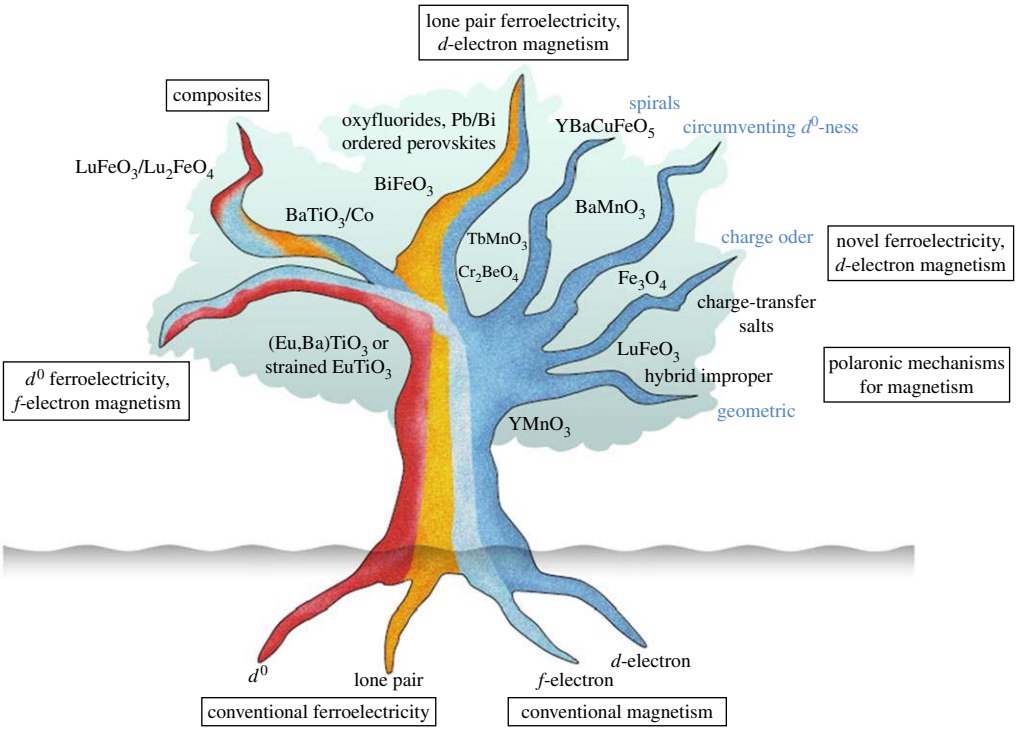

Figure 6. The 'Multiferroic Tree' that depicts how one can design multiferroics from the basic elements of bringing together magnetic species (for example, ions with f/d-electrons) and polar species (i.e. chemical species that lead to the emergence of a spontaneous polarization). Each branch depicts exemplar multiferroic systems; the boxes on the outside identify the dominant mechanism responsible for the formation of multiferroics [21]. (Online version in colour.)

early days regarding the magnitude of the spontaneous polarization (which was experimentally measured in epitaxial thin films to be approx. 90 µC cm^{-2} and confirmed theoretically [37]), it is now well established. In parallel with the scientific debate on the ferroelectric properties, there was an equal degree of debate as to the state of magnetism, particularly because it is complicated not only by the fundamental spin–orbit coupling physics but also from domain walls that exhibit enhanced magnetic moments. Although the ground state is a robust G-type antiferromagnetic structure (which can be described by spins in {111} that are ferromagnetically coupled in-plane but antiferromagnetically coupled out of plane along the [111]), the magnetic structure is quite a bit more sophisticated. As a consequence of the antisymmetric Dzyalozhinski–Moriya coupling (which is symmetry allowed for the *R*3*c* crystal symmetry), a small canted moment arises, which lies in the {111} (i.e. perpendicular to the spontaneous polarization direction). In single crystals, this canted moment spirals about the [1–9] so that it does not exhibit a macroscopically measurable magnetic moment until this spin spiral is broken, either by elastic strain (for example, through epitaxial thin-film growth) or through the application of a magnetic field of approximately 16–18 T [38]. Ferroelectric domain walls can play a key role in the emergence of a magnetic moment, which typically manifests in the form of a spin glass [39], described in figure 8. The underlying ferroelectric domain structure can be manipulated through the deposition rate to form well-ordered stripe domains (at low deposition rates) and a more mosaic-like domain structure at high deposition rates (figure 8*a–c*). The mosaic-like domain structure incorporates a high density of 109° domain walls, which exhibit spin frustration and an enhanced magnetic moment. As a consequence of this, BFO films with such a domain structure also couple strongly to a ferromagnet, leading to an enhanced exchange bias arising from the pinned uncompensated spins at the domain walls (figure 8*d–f*). Subsequent to this original work, some systematic studies

Table 1. This table complements figure 6. It summarizes the various identified mechanisms for creating multiferroics and magnetoelectrics.

pathway	fundamental mechanism	example systems
A-site driven	stereochemical activity of lone pairs on A-site leads to ferroelectricity; magnetism from B-site	$BiFeO_3$; $BiMnO_3$
geometrically driven	long-range dipole–dipole interactions and oxygen rotations breaks inversion symmetry	$YMnO_3$; $BaNiF_4$, $LuFeO_3$
charge ordering	non-centrosymmetric charge ordering leads to ferroelectricity in magnetic materials (e.g. Vervey transition)	$LuFe_2O_4$
magnetic ordering	ferroelectricity induced by a lower symmetry ground state that breaks inversion symmetry	$TbMnO_3$; $DyMnO_3$
atomically designed superlattices	still under investigation; likely lattice mediated	$LuFeO_3$–$LuFe_2O_4$
vertical epitaxial nanocomposites	coupling mediated by three-dimensional interfacial epitaxy, e.g. Spinel-Perovskite	$CoFe_2O_4$–$BiFeO_3$ $NiFe_2O_4$–$BiFeO_3$ $CoFe_2O_4$–$BaTiO_3$

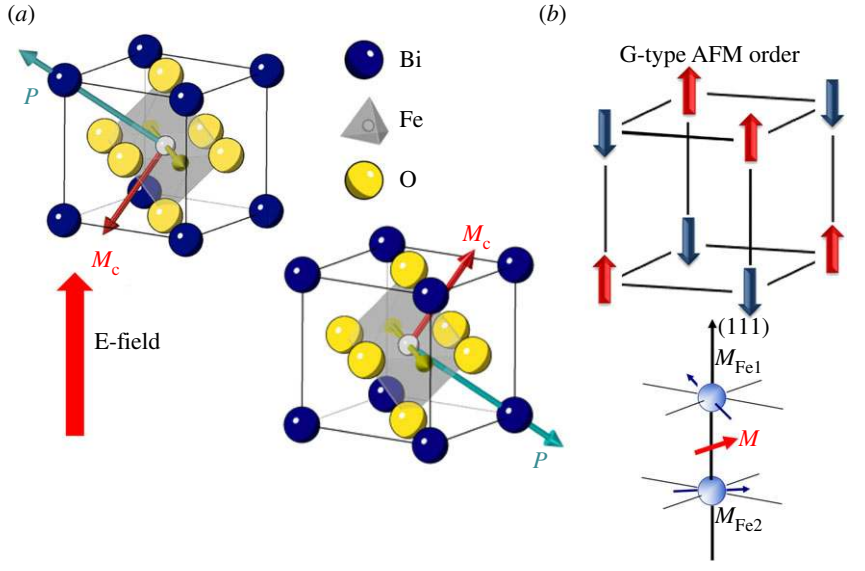

Figure 7. (*a*) A schematic illustration of the rhombohedral crystal structure of $BiFeO_3$ as well as the 180° switching of the polar axis and the associated changes in the canted moment direction ; (*b*) the G-type antiferromagnetic order and the canted moment arising as a consequence of the Dzyalozhinski–Moriya coupling. (Online version in colour.)

to create ordered arrays of 71° and 109° walls [40] led to a better resolution of the role of pinned uncompensated spins at such domain walls, leading to an exchange bias coupling to a ferromagnet. This is illustrated in figure 9.

The role of isovalent and aliovalent chemical substitutions at both the bismuth and iron sites has been extensively studied [36,37]. Outside of the fundamental understanding of the polar and

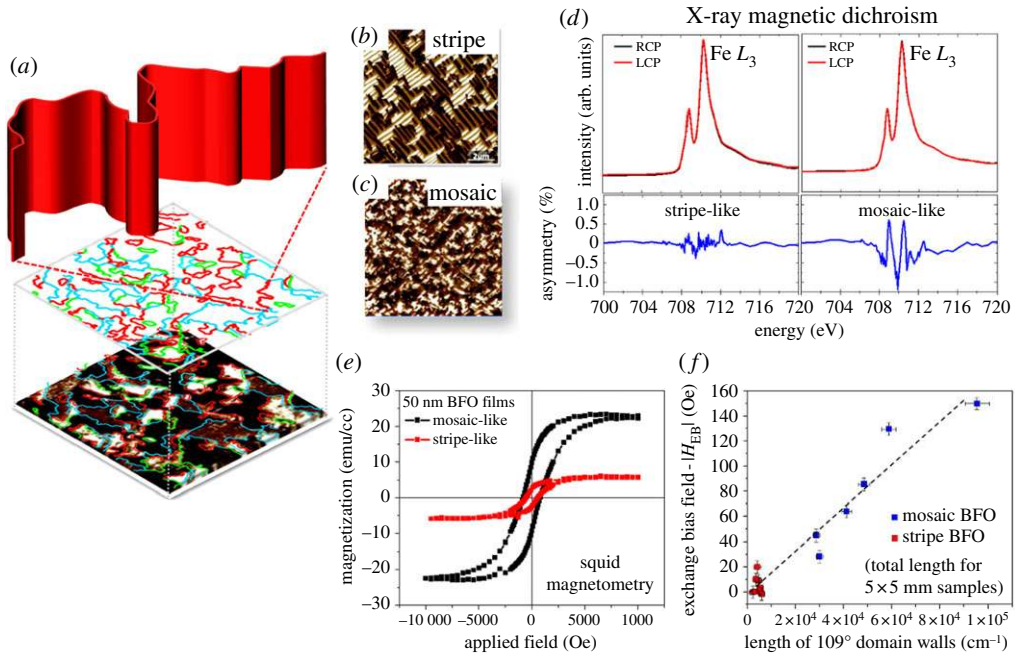

Figure 8. (*a*) An in-plane piezoforce microscopy (PFM) image (bottom) of a $BiFeO_3$ (BFO) thin film with a large density of 109° and 180° domain walls as illustrated by the detailed analysis (middle); a magnified schematic of the tortuous nature of the 109° wall is shown on top; (*b*) an in-plane PFM image of a BFO layer grown at a low deposition rate on a $SrTiO_3$ substrate showing two orthogonal sets of 71° domains; (*c*) when the same film is deposited at a faster rate, the domain structure progressively takes on a mosaic-like structure, as also shown in (*a*); (*d*) X-ray absorption spectra (XAS) and magnetic circular dichroism (XMCD) for the stripe-like and mosaic-like domain patterns, which show measurably different XMCD, indicating the role of 109° domain walls in enhancing the magnetic response of the film, as also revealed by magnetic measurements shown in (*e*); (*f*) plots the exchange bias field, H_{EB} of the BFO layer with a CoFe layer deposited on top, showing the systematic increase in the H_{EB} with the density of 109° domain walls. These results point to the existence of pinned uncompensated spins at the 109° domain walls. (Online version in colour.)

magnetic order, these studies have also focused on the possibility of creating phase boundaries (much like the morphotropic phase boundary in the $PbZr_{1-x}Ti_xO_3$ family of ferroelectrics) that can lead to large piezoelectric responses and allow for tuning of the ferroelectric switching behaviour [41–43]. Chemical substitutions at the Fe^{3+} site (e.g. Mn^{3+} or Co^{3+}) have mainly attempted to manipulate the antiferromagnetic nature [44]. While these studies have indicated a certain degree of success, detailed studies of the magnetoelectric coupling in such alloyed $BiFeO_3$ materials are still lacking. Indeed, a grand challenge would be to discover pathways to enhance the magnetic moment to approximately 50 emu cc^{-1} (the canted moment in pure $BiFeO_3$ is only approx. 6 emu cc^{-1}) while at the same time demonstrating magnetoelectric coupling. In this regard, Co-doping at the Fe-site has been shown to enhance the saturation moment to approximately 80 emu cc^{-1} [45,46]. Verification of these observations with theoretical studies as well as by other synthesis routes would be valuable. Similarly, a robust ferroelectric state as well as strong magnetoelectric coupling in such systems is still lacking and should be an active topic of research.

Thin-film synthesis of $BiFeO_3$ (and other multiferroics) has been a very fruitful pathway to study the materials physics of magnetoelectric coupling as well as pointing the way to possible applications. The perovskite symmetry and lattice parameters (pseudocubic lattice parameter of 3.96 Å) close to a large number of oxide-based substrates means that epitaxial synthesis is possible and has indeed been demonstrated. Films with thicknesses down to just a few unit cells and as large as a few microns have been synthesized by physical-vapour deposition (e.g. pulsed laser

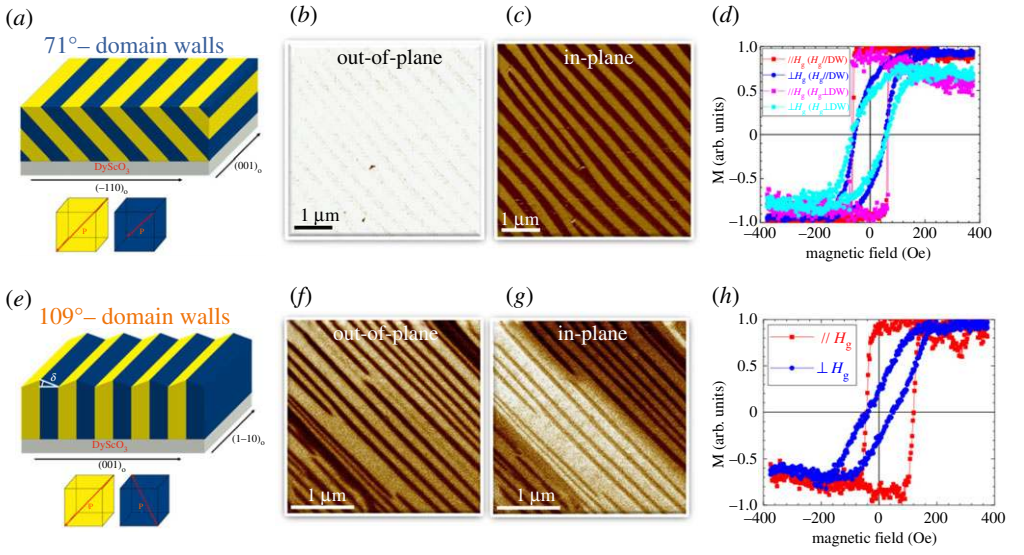

Figure 9. (*a*) A schematic of ordered arrays of 71° domain walls in the $BiFeO_3$ layer, which can be created through epitaxial growth on a $DyScO_3$ substrate with a thin (approx. 5–10 nm) of $SrRuO_3$ as the bottom electrode, as shown by the PFM images in (*b*,*c*); (*d*) Magnetization (M)-magnetic field (H) loops for a 2 nm CoFe layer deposited on such a 71° domain wall array, both parallel and perpendicular to the direction in which the magnetic field (2000e) was applied during growth; (*e*) a schematic of an array of 109° domain walls in the BFO layer, which is grown without the bottom SRO layer, as illustrated in the PFM images in (*f*,*g*); (*h*) the M-H loops for the CoFe layer deposited on such a 109° domain wall array, showing a clear indication of exchange bias (red loop) due to the existence of pinned uncompensated spins at the 109° domain walls. (Online version in colour.)

deposition, sputtering, molecular beam epitaxy), chemical-vapour deposition [47] and chemical-solution deposition. Many studies have used conducting perovskite electrodes (such as $SrRuO_3$, $La_{1-x}Sr_xMnO_3$, $La_{1-x}Sr_xCoO_3$) as bottom electrodes to both template the perovskite phase as well as provide a bottom contact for electrical measurements. These synthesis studies have led the way to enable a wide range of materials physics studies including thickness-size effects down to just a few unit cells [48]. Consistent with other perovskite ferroelectrics, a suppression of the magnitude of the polar order is observed, although both theory and experiments indicate that a polar state is stable down to even a couple of unit cells.

Using epitaxy as a building block, one can start to explore magnetic and magnetoelectric coupling between an oxide ferromagnet (such as La–Sr–Mn–O [LSMO]) and $BiFeO_3$. The ability to grow such atomically perfect heteroepitaxial using techniques such as molecular beam epitaxy and RHEED-assisted pulsed laser deposition have been instrumental in enabling the study of magnetism across such interfaces, as illustrated in figure 10. *In situ* probes, such as time of flight-ion scattering and recoil spectroscopy (TOF-ISARS) indeed show that the interface termination can be manipulated at the scale of the individual perovskite building blocks, namely the A–O plane or the B–O_2 plane as shown by the atomic resolution images in figurey 11*c*,*d*. This is accomplished by inserting a 1.5–2.5 unit cell thick layer of $SrRuO_3$ (SRO) on the TiO_2-terminated $SrTiO_3$ substrate surface. Deposition of two–3 unit cells of SRO on the substrate followed by a short wait (3–5 min) enables the desorption of the topmost Ru-layer, thus converting the RuO_2-terminated surface to a Sr–O-terminated surface; this Sr–O-terminated surface then seeds epitaxial growth of the LSMO layer and converts the MnO_2 termination to a La(Sr)–O termination, as shown by the TOF-ISARS spectra in figure 10*b*. We get back to the issue of magnetoelectric coupling in such model interfaces after a short summary of theoretical approaches.

From a theoretical perspective, while first principles density functional theory calculations remain central for understanding and predicting the properties of multiferroics, second-principles

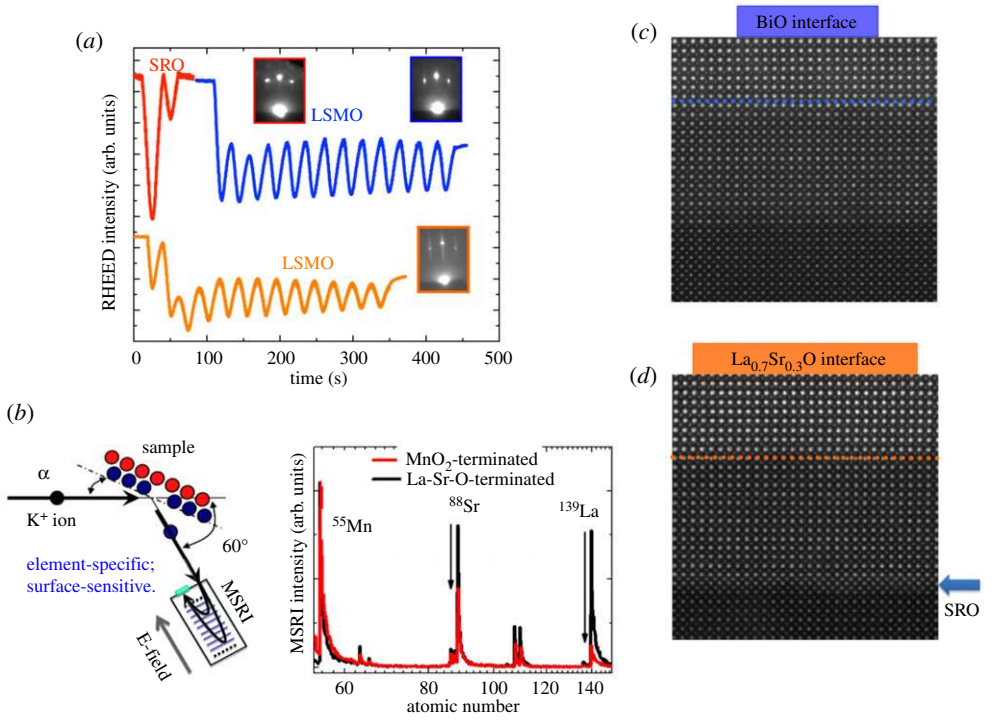

Figure 10. Synthesis of Model Systems. This figure illustrates epitaxial synthesis as a pathway to create model systems at the scale of a single unit cell. (*a*) A RHEED pattern of the growth of the LSMO bottom electrode on a TiO_2-terminated $SrTiO_3$ substrate; insertion of two unit cells of $SrRuO_3$ leads to a conversion of the termination from B-site to A-site; (*b*) Time of flight-ion scattering and recoil spectroscopy (TOF-ISARS) of the two types of substrate surfaces. The spectra are normalized to the Mn peak, and it is clear that the La content for one of them (black) is much higher than that of the other (red); (*c*,*d*) atomic resolution STEM images of the two types of interfaces showing that atomically sharp interfaces can be obtained. (Online version in colour.)

calculations with embedded model Hamiltonians are proving increasingly valuable in the study of larger systems, for example, heterostructures, domain walls and defects, as well as longer time scales in molecular dynamics. They have been applied to describe structural phase transitions of prototypical ferroelectrics [49,50], and recent extensions to include additional lattice degrees of freedom [51], as well as magnetic interactions [52], have extended their applicability to multiferroics. For example, an effective Hamiltonian consisting of a lattice part incorporating ferroelectric distortions, octahedral rotations and strain, a contribution from the interaction of the magnetic moments with each other, and coupling between the magnetic moments and the lattice, has been shown to accurately reproduce the crystal and magnetic structures of bulk BFO. On a larger length scale, a Landau–Ginzburg thermodynamic potential that includes both polar and anti-polar distortions and their coupling to magnetism has been successful in reproducing the bulk behaviour of BFO and offers great promise for predicting properties in thin-film heterostructures and nanostructures [53]. Multi-scale approaches that allow treatment of the electronic and lattice degrees of freedom on the same footing [54] could lead to vastly enhanced system size and accuracy when combined with improved tools for generating effective potentials using input from first principles [55]. Modelling of the dynamics of ferroelectric switching [56] and its effect on magnetic order [57], both of which are on time- and length scales that are far outside the ranges accessible using density functional methods, has now become feasible. Such models in combination with molecular dynamics start to allow calculation of dynamical magnetoelectric responses in the THz region [58], which is particularly timely as it coincides with advances in experimental methods for generating THz radiation [59]. Finally, the

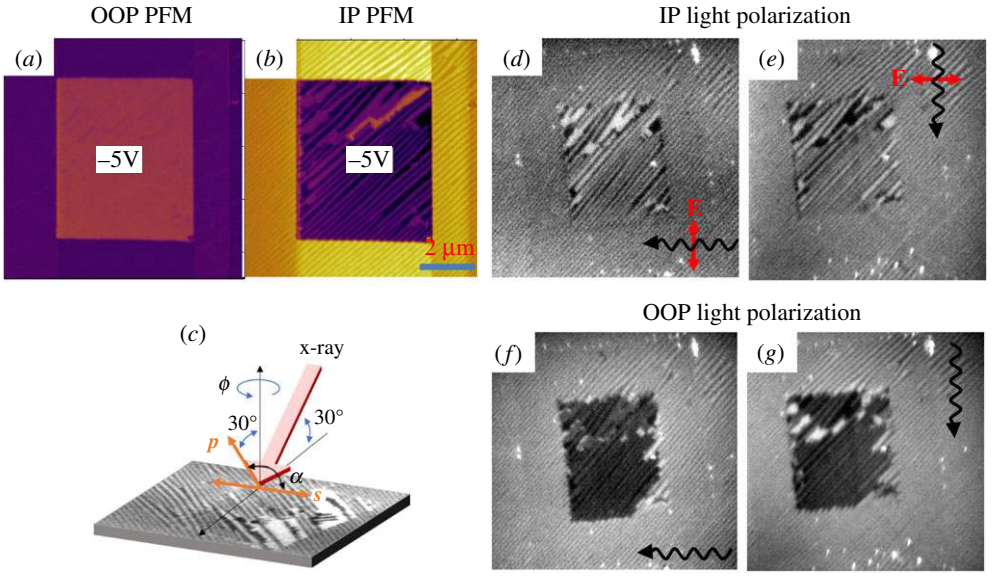

Figure 11. Electric field control of AFM probed using XLD-PEEM. On the left (*a*,*b*) is PFM showing the ferroelectric domain structure before and after switching; (*c*) a schematic that illustrates the XMLD-PEEM imaging process; (*d*,*e*) XMLD-PEEM images of a switched region with light polarization in-plane (IP) with two orthogonal azimuthal angles; (*e*,*f*) similar images obtained with the light polarization out of plane (OOP). (Online version in colour.)

possibility of magnetoelectric multipole as an order parameter for phase transitions that break both space-inversion and time-reversal [60,61] seems intriguing, although not fully explored experimentally.

With this basic understanding of the order parameters and symmetry in systems such as BFO, we can now ask the most important question: How does magnetism couple to an electric field and how can the state and direction of magnetism be manipulated through the application of an electric field? In nature, this coupling between electricity and magnetism occurs through electromagnetism. However, in order to be able to dramatically change the state of magnetism with an electric field, it is desirable for the magnetoelectric coupling to be significantly stronger than what is available in nature.

Understanding electric field control of AFM in BFO requires probing AFM using X-rays or neutrons. Such studies of $BiFeO_3$ have shown that when the polarization state switches with the application of an electric field, there is a corresponding rotation of the magnetic order [62,63]. Such a change can also be spatially probed using a combination of piezoresponse force microscopy (to image the ferroelectric order) and X-ray magnetic linear dichroism (XLD) photoemission electron microscopy (PEEM) (to image the antiferromagnetic order) (figure 11). It is interesting to note that there has been little detailed work on a full understanding of the dynamics of the manipulation of the AFM state by an electric field, with most studies assuming the magnetic order merely follows that of the polar order, but not clarifying that pathway. This is an opportunity for future ultra-fast dynamics research, because the antiferromagnetic resonance frequencies are in the several hundred GHz range and $BiFeO_3$ has ferroelectromagnons in the 700 GHz to 1 THz range. Given the current surge in interest in antiferromagnetic spintronics, such insulating multiferroics would also garner more interest.

(a) Electric field control of mixed magnetic states and nanocomposites

Early on in the evolution of the modern version of multiferroics and magnetoelectrics [64], it was realized that nanocomposites comprising ferrimagnets embedded (in many cases epitaxially) in

a ferroelectric/piezoelectric matrix could lead to efficient magnetoelectric coupling controlled by interfacial epitaxy. Such nanocomposites, exemplified by single crystalline nanopillars (figure 12*a*) of ferrimagnetic spinels (e.g. $CoFe_2O_4$) embedded epitaxially in a ferroelectric perovskite matrix (e.g. $BiFeO_3$), are illustrated in the AFM images (figure 12*b*). The epitaxial nature of the lateral interfaces is shown in the corresponding planar section TEM images (figure 12*c*). Electric field-driven switching studies reveal perhaps the most interesting aspects of such nanocomposites of relevance to deterministic switching of the magnetic state with an electric field. While the initially magnetized state (figure 12*d*), can be switched with an electric field, only approximately 50% of the magnetic nanopillars switch their state (for example, from magnetization pointing up to down; figure 12*d*,*e*). Detailed analysis of these data [65] shows that this is indeed true and is a direct consequence of the fact that the electric field assists in manipulating the magnetic anisotropy of the ferrimagnetic nanopillar through the epitaxial interface between the perovskite ferroelectric and spinel ferrimagnet. However, the magnetic anisotropy of the nanopillar is the same whether it is magnetized up or down (along the long axis of the nanopillars), thus leading to a approximately 50/50 mixture of up/down states after the electric field is applied. This study also throws light on the most important physics of such coupling phenomena, namely that switching the magnetization direction in a deterministic fashion, i.e. by 180°, requires that there be a field that breaks time-reversal symmetry. However, the electric field and corresponding piezoelectric stress that is generated does not break time-reversal symmetry and thus cannot deterministically switch the magnetization, but can indeed alter, during the switching process, the magnetic anisotropy. This is further supported by the observation that the application of a small magnetic field to the nanopillar arrays during the electric field-induced switching event leads to a complete switching of their magnetic state [60]. These results also point to the need to have a coupling mechanism that is magnetic in nature, for example, interfacial exchange bias coupling, which we focus on next.

(b) Electric field control of magnetization direction through interfacial exchange coupling

There are a few possible manifestations of electric field control of magnetism; the review by Song *et al*. [20] provides a complete summary of these pathways. The first pathway would be to manipulate the direction of magnetization, while the magnitude remains essentially unchanged; another approach would be to manipulate the magnitude of the net, macroscopic magnetization, for example, through a ferromagnetic to an antiferromagnetic phase change [66–70]. A third pathway would manipulate the magnetic anisotropy, for example, using strain, as already illustrated by the nanocomposite example in figure 12. From a practical perspective, especially in terms of carrying out logic-in-memory operations with spins [1,10], it is most useful if the direction of magnetization can be robustly switched. Perhaps the most significant breakthrough in the past few years is the demonstration that the magnetization direction in conventional ferromagnets (e.g. $Co_{1-x}Fe_x$) can be rotated by 180° with an electric field [71,72] when it is exchange-coupled to $BiFeO_3$. The extension to all-oxide $La_{0.7}Sr_{0.3}MnO_3/BiFeO_3$ interfaces (figure 13), with chemically abrupt *A*-site termination [74], allowed for electric field control of exchange bias coupling at temperatures below 100 K [73].

Earlier work on the same system has shown the ability to reversibly switch between two exchange-biased states with the same polarity (unipolar modulation) without the need for additional magnetic or electric fields in a multiferroic field effect device, but eventually the ability to reversibly switch between these two states with opposite polarity (bipolar modulation) was demonstrated as well (figure 13). The key was modifying the direction of the magnetization in the $La_{0.7}Sr_{0.3}MnO_3$ with respect to the current in the device channel. A reversible shift of the polarity of exchange bias through the zero applied magnetic field axis was thus achieved with no magnetic or electric field cooling and no additional electric or magnetic bias fields: in essence, full direct electric field control of exchange bias. This also helped clarify the mechanism underlying the change in exchange bias coupling.

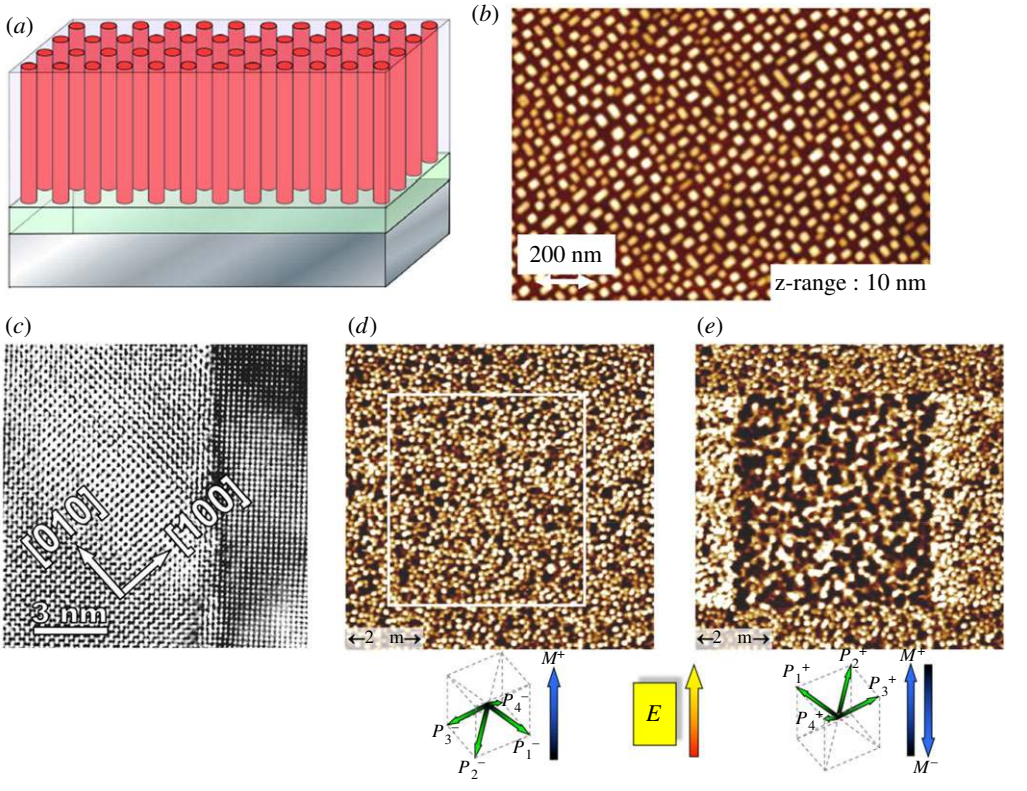

Figure 12. (*a*) A schematic of the three-dimensional vertically epitaxial magnetoelectric nanocomposite; (*b*) AFM image of the ferrimagnetic $CoFe_2O_4$ nanopillars (in bright contrast) embedded in a ferroelectric $BiFeO_3$ matrix (in dark contrast); (*c*) A high-resolution STEM image of the interface between the spinel ferrimagnet and the perovskite ferroelectric; (*d*) a magnetic force microscopy (MFM) image after magnetization at 2 T, in which the ferrimagnetic nanopillars appear in bright contrast; (*e*) the corresponding MFM image after the matrix was switched with a −16 V applied with an AFM tip. The schematics below describe the magnetic state before and after the electric field switching. (Online version in colour.)

An important open problem is the development of oxide ferro- or ferri-magnets with high T_c, a significant remanent moment and strong exchange coupling and Ohmic contacts with $BiFeO_3$ or other multiferroics; spinels or double perovskites are promising candidates in this regard [75,76]. In a complementary direction, the antiferromagnetic domain orientation in magnetoelectric Cr_2O_3, which can be controlled by an electric field, has been shown to affect the exchange-bias coupling to a ferromagnetic overlayer [66] opening a pathway to electric field switchable exchange-bias devices.

(c) Manipulating magnetic state (or magnitude of the magnetization) with an electric field

In parallel to these efforts to control the direction of magnetization with an electric field, there have been successes in electric field manipulation of the magnetic state (or the magnitude of the net macroscopic magnetization), for example, by switching between ferromagnetism and AFM using composites [67]. One example is electric field modification of the magnetic exchange interactions in magnetic $Fe_{1-x}Rh_x$ heterostructured with piezoelectric $(1-x)Pb(Mg_{1/3}Nb_{2/3})O_3-xPbTiO_3$. Motivated by the volume change at the ferromagnetic to antiferromagnetic transition in $Fe_{1-x}Rh_x$ [68,69], an electric field was used to drive the reciprocal effect, a ferromagnet-to-antiferromagnet transition induced by a structural deformation [70,77]. Because the resistivities of the two magnetic phases differ, the magnetic transition is accompanied by an approximately

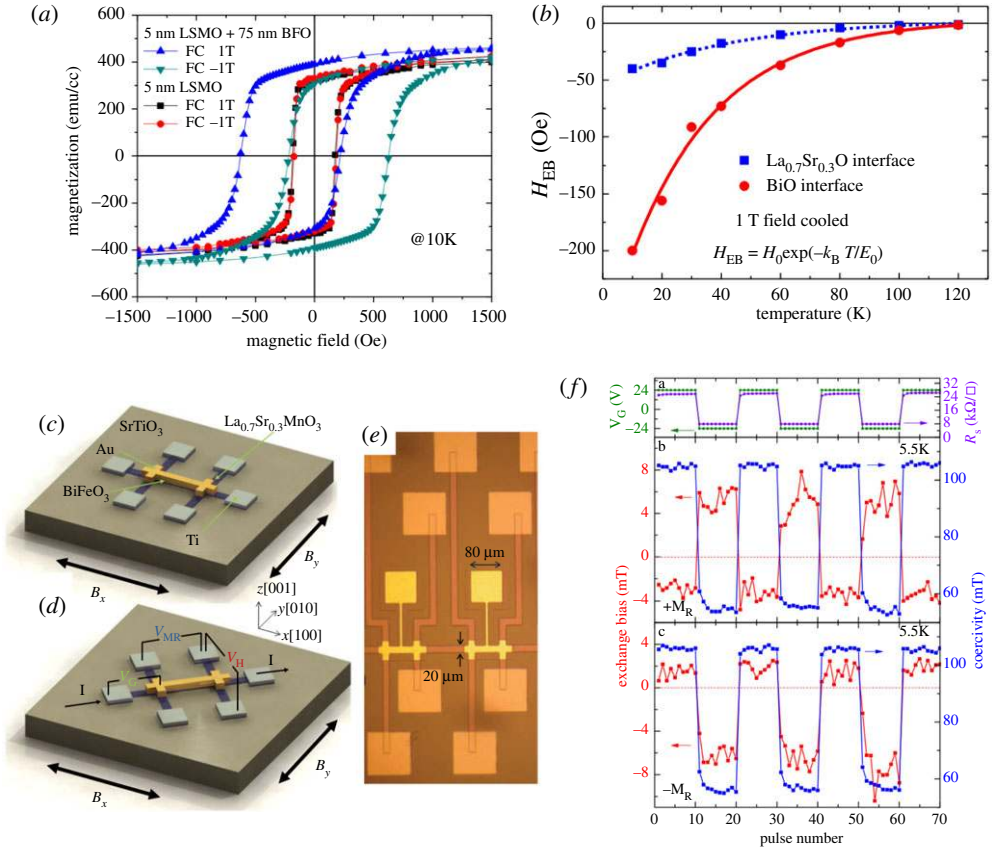

Figure 13. Electric field manipulation of interfacial magnetic coupling in epitaxial heterostructures. (*a*) 1 T, field-cooled magnetic hysteresis loops at 10 K showing a strong exchange bias of 200Oe for a 5 nm LSMO-75 nm BFO heterostructure; (*b*) the magnitude of the exchange bias field as a function of temperature and interface termination (La/Sr–O versus Bi–O interfaces); (*c*,*d*) device layouts for magnetoelectric measurements, with the corresponding SEM image shown in (*e*); (*f*) the bipolar voltage profile and the corresponding exchange bias and coercivity showing full electric field switching of the exchange bias [73]. (Online version in colour.)

25% change in film resistivity. Open challenges include reducing the optimal working temperature from around 100°C to room temperature, tuning the chemical composition to optimize the strengths of the exchange interactions, achieving complete conversion between the ferromagnetic and antiferromagnetic phases and reducing the required applied voltages. Other promising systems are the Mn-Pt intermetallics and half-doped perovskite manganites such as $La_{0.5}Sr_{0.5}MnO_3$, in which an electric field-driven charge-ordered antiferromagnetic insulator to ferromagnetic metal transition could be possible [78].

6. Ultra-low power logic-memory devices based on multiferroics

A large number of pathways are currently being explored to create low power non-volatile memories within the context of next-generation computing (e.g. [1,2,11]). A full description of these various pathways is a dedicated review in itself and is not the prime focus of this review. Instead, we will attempt to capture the state of the art of various approaches after a brief summary of the magnetoelectric and multiferroic approaches.

The push for ultra-low power logic-memory devices builds from seminal observations of the potential of magnetoelectric control using multiferroics, the key being the ability to control

magnetism with electric field at room temperature [79] using a spin-valve device (figure 14*a*) to demonstrate the coupling. Efforts in this direction are currently being undertaken. For example, magnetoelectric switching of a magnetoresistive element was recently shown to operate at or below 200 mV, with a pathway to get down to 100 mV [80]. The fact is that the voltage (which is relevant from the device perspective) and the electric field (which drives the switching physics) means that reducing the thickness is an obvious pathway to get to such low voltages. A combination of structural manipulation via lanthanum substitution and thickness scaling in multiferroic $BiFeO_3$ has helped to scale the switching energy density to $\approx 10\,\mu J\,cm^{-2}$ and provides a template to achieve attojoule-class non-volatile memories. Lanthanum substitution is known to both lower the polarization and the ordering temperature (and therefore the energy of switching) of the ferroelectric and to take advantage of innate thickness scaling effects (thinner films require smaller voltages for switching) [38]. Using this approach, it was possible to show that the switching voltage of the giant magnetoresistance (GMR) response can be progressively reduced from ≈1 V to 500 mV by a reduction of the film thickness down to 20 nm (figure 14). Robust electric-field control of the magnetization direction in the bottom $Co_{0.9}Fe_{0.1}$ layer was shown in measurements both in a magnetic field of 100 Oe as well as in the remanent state (i.e. zero magnetic field) (figure 14*b*,*c*). The low-voltage magnetoelectric switching in multiferroic $Bi_{0.85}La_{0.15}FeO_3$ was further probed by XMCD-PEEM imaging at the Co L_3 edge via studies (inset, figure 14*d*,*e*), where application of ±500 mV revealed contrast changes consistent with reversal of the in-plane magnetization [79].

Building from such observations, a promising recently developed logic-memory architecture [1] brings together the inverse Rashba–Edelstein (spin-Hall) effect (IREE) [81–84] and electric field control of magnetism using a multiferroic. The resulting magnetoelectric, spin–orbit coupled logic device (MESO) [10] (figure 15) uses the IREE effect to convert spin to charge (or voltage) and the multiferroic to perform the opposite conversion of charge to spin. Success of the device rests on an increase in the IREE voltage output from current values of hundreds of μV to hundreds of mV as well as a reduction in voltage requirement for the magnetoelectric component from the current value down to approximately 100 mV. Such breakthroughs could lead to a transformative 1 aJ (10^{-18} J) per memory bit or logic element, illustrated schematically in figure 15 [10].

Despite all of the prior work, switching a ferroelectric state (as well as a multiferroic state) with a voltage as small as 100 mV remains a challenge and a research opportunity. Because the electric field scales with the dimensions of the ferroelectric, progression towards switching voltages of 100 mV automatically require that either the switching field is very low or that the switching behaviour scales well with thickness. Therefore, it is critical to understand ferroelectric switching behaviour in the ultra-thin limit (less than 20 nm). Quantitative studies of the switching dynamics at such a thickness are still lacking and should be a fruitful area of research especially on the experimental side. What are the limits to the switching speed of ferroelectrics/multiferroics? There have been speculations that one limit could be acoustic phonon mode (i.e. the velocity of sound in the material) as the switching of the polar state clearly involves the time-dependent deformation of the lattice. For nominal values of the velocity of sound in such oxides (approx. $3000\,m\,s^{-1}$), this would suggest a switching time of the order of a few tens of picoseconds. Thus, the role of lattice dynamics during the dipolar switching event needs considerable further work. Measuring at such time scales requires very fast electronics (e.g. pulse generators with rise times smaller than a few tens of picoseconds and oscilloscopes that can capture the switching transients as commensurate speeds); thus, it is not surprising that there have been only a few measurements of the polarization switching dynamics approaching such time scales [85]. This is true for both ferroelectrics and multiferroics [86] and as we go forward into this exciting field of electric field controlled magnetic devices, such studies are critically needed.

An equally important aspect is the stability of the polar state as the thickness is scaled down. Such size effects have been extensively studied in classical ferroelectrics [87] and are characterized by a suppression of the order parameter as the thickness is scaled down. Similar studies have been undertaken in the case of the $BiFeO_3$ system, albeit in an incomplete sense. Several studies have shown that the polar order parameter is suppressed, but still maintained; The antiferromagnetic

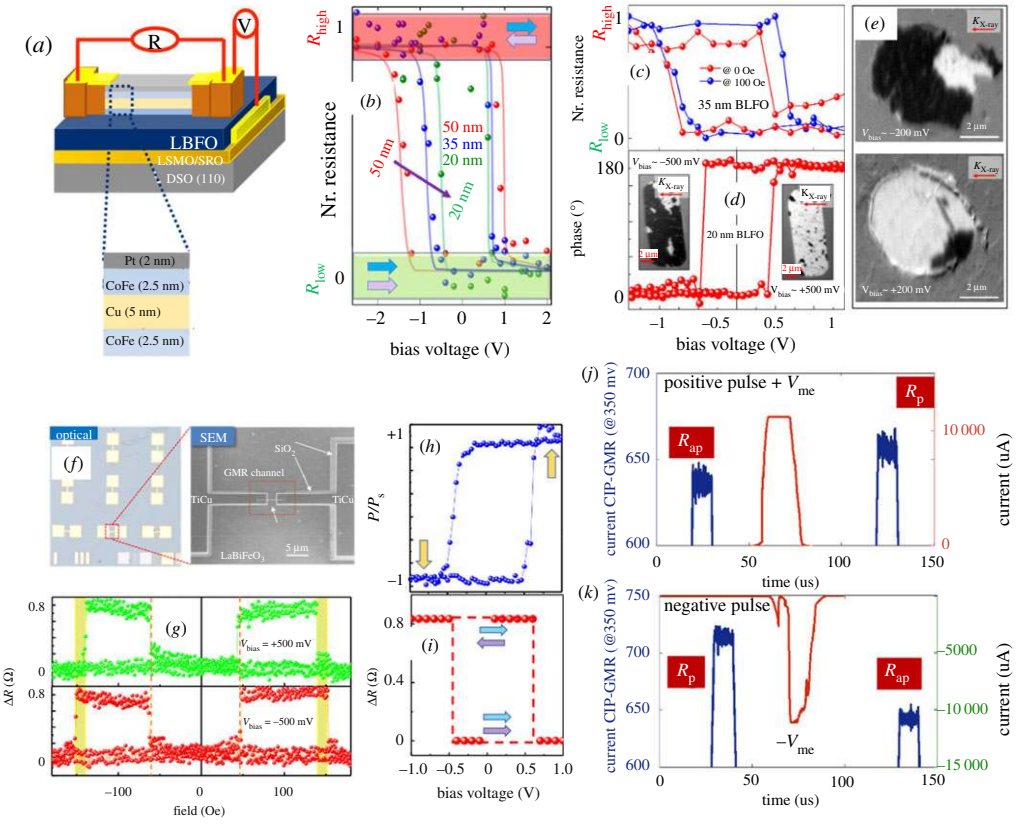

Figure 14. (*a*) A Schematic of the magnetoelectric test structure comprised a CoFe–Cu–CoFe spin valve in contact with the La-BFO surface; (*c*) voltage-dependent GMR hysteresis as a function of La-BFO thickness from 50 nm down to 20 nm; (*b*) the normalized resistance of the GMR stack as a function of applied voltage at zero field (red) and at 1000e (blue); (*d*) the corresponding piezoelectric phase data showing switching of the polar state at approximately 500 mV for the 20 nm LBFO layer; also shown are the corresponding XMCD-PEEM (at the Co-edge) for a CoFe dot that has been switched (from black to white) with a bias of 500 mV; (*e*) the corresponding XMCD-PEEM data for a CoFe dot on a 10 nm LBFO layer showing switching at approximately 200 mV (adapted from ref. [79]); (*f*) a composite of optical and SEM images of approximately 100 nm GMR spin-valve channels fabricated using e-beam lithography; (*g*) the corresponding resistance change versus magnetic field for both +500 mV and −500 mV applied electric field; (*h*) the normalized ferroelectric loop for the La-BFO and (*i*) the corresponding normalized GMR resistance as a function of applied voltage; (*j*,*k*) the GMR resistance for the parallel (R_p) and antiparallel (R_{ap}) states measured with 20 µs electric field pulses. (Online version in colour.)

order has also been shown to exist at room temperature in films that are as thin as 4 nm (10 unit cells). What has not been shown is the coupling between the two order parameters at such length scales, and more importantly, electric field manipulation of this coupling. Thus, a deeper, quantitative understanding of the stability of the individual order parameters, the coupling between them as well as E-field manipulation of this coupling at a thickness less than approximately 10 nm, would be of significant interest.

While challenges at these voltage/energy, length and time scales exist for all ferroelectric materials, special attention is now being given to such responses in multiferroics such as BFO. The ferroelectric switching process in BFO is believed to be limited by nucleation and growth of reverse domains [88] broadly captured by the Kay–Dunn model [89], in which the coercive field scales as film thickness $d^{-2/3}$. Consequently, progressively larger reductions in film thickness are needed to reduce the coercive voltage as it is pushed to smaller values. In BFO, lanthanum substitution has been shown [90] to reduce the switching energy by reducing the polarization

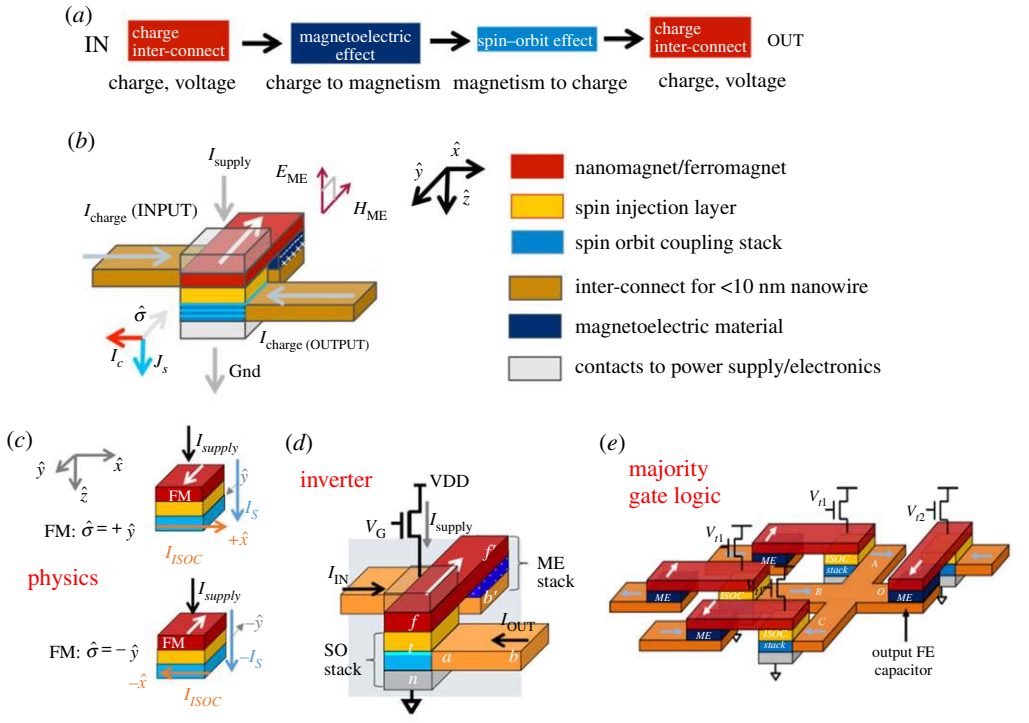

Figure 15. (*a*) A schematic that illustrates how the magnetoelectric, spin–orbit (MESO) device works; the input voltage signal is converted into a spin signal by the magnetoelectric layer; the logic operation is then carried out and the spin–orbit layer converts this back to a voltage signal, which is easier to read out compared with a spin signal; (*b*) a schematic of an individual MESO element comprised the various layers shown to the right; (*c*) depicts the fundamental physics behind the MESO device, in which the direction of the ferromagnetic layer (in red) sets the direction of the direction of the spin–orbit coupled current; (*d*) a schematic of how the basic MESO building block is used to make an Inverter (which is a fundamental unit for logic operations) and (*e*) depicts how a majority gate logic is constructed from the MESO device (figure adapted from ref. [10]). (Online version in colour.)

[48], although to an insufficient extent to date. Pushing $BiFeO_3$ close to a phase boundary between ferroelectric and antiferroelectric states or identifying materials without the octahedral rotations of BFO could be an alternative pathway to smaller coercive fields. The challenges facing the spintronics community in enhancing the output of the inverse Rashba–Edelstein effect component by two to three orders of magnitude [91] are equally exciting.

Several important considerations towards carrying out such quantitative measurements need mentioning. First, dielectric leakage becomes an ever-increasing component at such thickness; an extreme case would be a 'shorting' of the test element. Thus, measurements at such thicknesses automatically mean that the test structures will have to be laterally quite confined (likely in the 50–100 nm range), thus requiring sophisticated lithography and definition. Second, interfaces will play an increasingly important role in determining both the stability of the polar state as well as transport across such small thicknesses. For example, interfacial Schottky barriers can significantly alter the potential drops across the sample and thus the voltages required to switch the polar state. Incomplete screening of the spontaneous polarization at the interface [92] can lead to its suppression. The role of point defects (both ionic and electronic) will become all the more important as we are now dealing with films of approximately 10 unit cell thickness.

Finally, figure 16 summarizes the state of the art of the various memory technologies (both mature technologies such as the NOR-FLASH, DRAM and SRAM) as well as emerging technologies and puts the magnetoelectric approach described in this review into perspective.

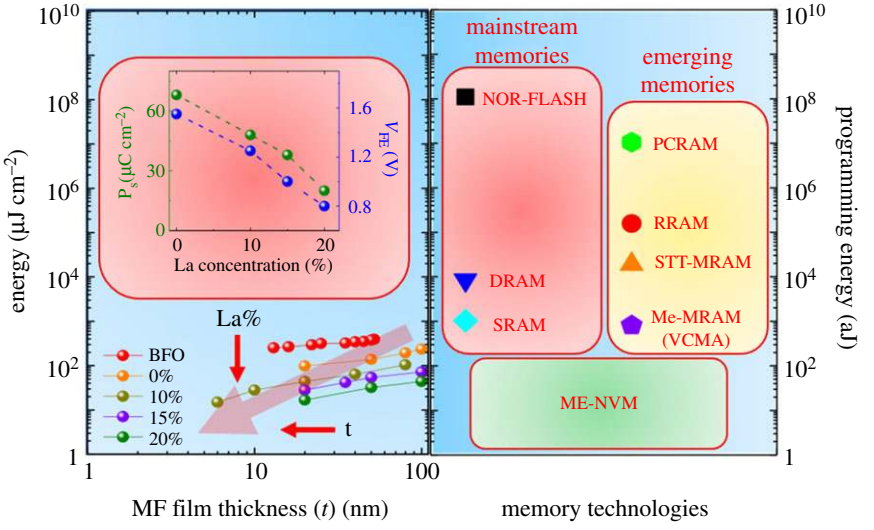

Figure 16. This figure captures the state of the art in tuning the switching voltage and spontaneous polarization of $BiFeO_3$ through La-substitution and film thickness at the Bi-site, which therefore leads to a reduction in the energy consumed (the left panel); the right side of the figure compares Mainstream memories (NOR-FLASH, DRAM and SRAM) to Emerging memories (PCRAM, RRAM, STT-RAM and ME-MRAM) as well as the magnetoelectric non-volatile memory-based logic (ME-NVM). (Online version in colour.)

As a broad conclusion, voltage-driven devices do offer the potential for a significant reduction in energy consumption compared with current-driven devices. Having said that, the recent developments in spin–orbit torque-based switching of the magnetic state offers significant promise for lowering the energy consumption, if the efficiency of spin-to-charge conversion is significantly enhanced.

7. Challenges and opportunities

It seems inappropriate to write a concluding section when, in reality, the exciting journey has just begun. Electric field control of the magnetization direction at room temperature is now clear with the voltage required to accomplish this dropping down to just 0.5 V. To get to an aJ switch, it is critical to reduce these switching voltages down even further (to at least 100 mV) in conjunction with a switching charge density of approximately 10 μC cm^{-2}. The key materials physics issues are captured in figure 17; at the broader level, table 2 summarizes some of the key basic science and translational issues to be addressed. How robust can this be, especially with respect to repeated cycling of the electric and magnetic states? In this regard, like in the field of ferroelectric thin films for memory applications, it appears that we need to increase the focus on the nature of the ferromagnet and its interface to the multiferroic. Prior experience with ferroelectric capacitors has shown that a conducting oxide contact yields a very robust capacitor; in a similar vein, we expect an oxide ferromagnet to form a more robust contact to the oxide multiferroic. Thus, there is an urgent need to discover and interface an oxide ferromagnet that couples magnetically to the multiferroic at room temperature. A template for this is already available from the work on $La_{0.7}Sr_{0.3}MnO_3/BiFeO_3$ interfaces, which display robust electric field control of the magnetization direction, albeit at 100 K. Can the double perovskites, such as $Sr_2(Cr,Re)O_6$ [74] with a high magnetic Curie temperature be possible alternatives to the LSMO system? In the same vein, there is an urgent need to discover more room temperature multiferroics so that one can explore multiple pathways to use these novel functionalities. Finally, searching for new room temperature multiferroics would be a very worthwhile pursuit for the

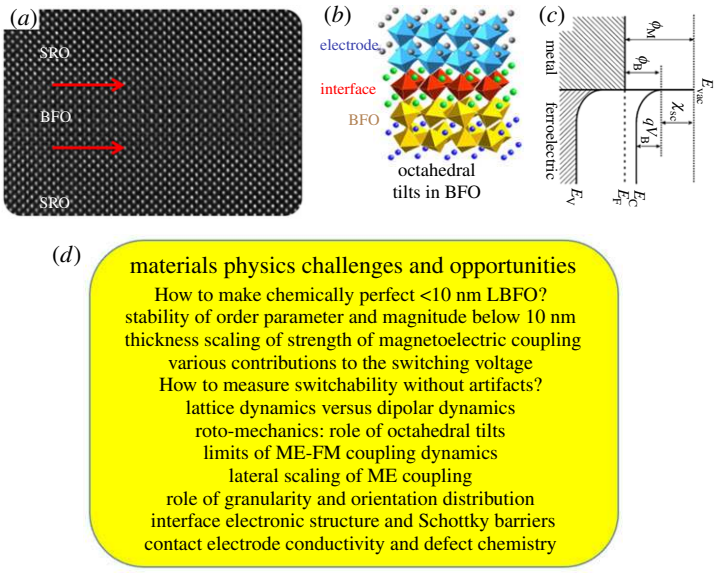

Figure 17. (*a*) An atomic resolution image of a six-unit cell thick $BiFeO_3$(BF) layer sandwiched between epitaxial $SrRuO_3$(SRO) top and bottom electrodes as a representative of sub-10 nm thick multiferroics as model systems; (*b*) is the corresponding crystal model showing the octahedral tilts (in both the SRO and BFO layers) as well as the possibility for the formation of interface Schotty barriers, shown in (*c*); (*d*) summarizes several key unanswered materials physics questions for such sub-10 nm multiferroics. (Online version in colour.)

materials community, especially when armed with the computational discovery platforms such as the Materials Genomics approach driven by ML pathways [93]. The confluence of crystal chemistry, computational discovery and atomically precise synthesis is a potent combination that has already been shown to lead to unexpected phenomena [94].

As mentioned in table 1, there is a lot of potential in designing magnetoelectrics at the atomic scale using epitaxial superlattices. The original work of Mundy *et al.* [34] on $LuFeO_3$–$LuFe_2O_4$ superlattices showed that the epitaxial pathway to magnetoelectric coupling is indeed possible. The work of Fan *et al.* [95] revealed the microscopic details of the coupling across the ferroelectric ($LuFeO_3$) ferrimagnet ($LuFe_2O_4$) interface. A key issue with $LuFe_2O_4$ is the fact that the Curie temperature is lower than room temperature (approx. 240 K in the bulk; approx. 280 K in epitaxial superlattices [34]). Thus, it would be desirable to replace this with other structurally and chemically compatible ferrites. Research in this regard is underway, using $CoFe_2O_4$ as the replacement for $LuFe_2O_4$ and publications outlining the coupling in such systems will be forthcoming.

In this sense, tremendous progress has been made in understanding chemistry–structure–property relationships, and in engineering specific atomic architectures, so that an era of 'multiferroic materials by design' is already underway. In particular, targeted functionalities, such as large magnetization and polarization and even exotic polarization topologies, are now within reach. Electric field control of magnetism, while demonstrated in multiple implementations, must be optimized so that it can be achieved with smaller voltages, ideally below 100 mV. For multiferroic devices to be technologically competitive will therefore require precise growth of ultra-thin films guided by theoretical studies to exactly define the chemical compositions needed to optimize the polarization and coercive field. This will require a greater fundamental understanding, which will be facilitated by improved first- and second-principles methods. Even with such a low-field-switching breakthrough, scale-up and integration, in particular compatibility with existing silicon processing methods, and integration with the appropriate

Table 2. A summary of challenges and opportunities both at the fundamental materials physics level as well as translation into technologies.

materials physics	translational
Discovery of new, room temperature multiferroics with robust coupling between magnetism and ferroelectricity, strong coupling and magnetic moment larger than 50 emu cc^{-1}	Achieving thermal stability of ferroelectric and magnetic order parameters, as well as robust coupling between them, in 10 nm length-scales at room temperature. Thus, careful measurements of magnetoelectric and multiferroic phenomena at such length scales is critical
Developing new mechanisms for magnetoelectric coupling and understanding and approaching the limits of the strength of such phenomena	Reducing the voltage required for ferroelectric/magnetoelectric switching to approximately 100 mV
Atomic-scale design and layer-by-layer growth as an attractive pathway to discover and synthesize new room temperature multiferroics	A second key requirement for ultra-low power electronics (e.g. an attojoule switch) would be designing proper ferroelectric multiferroics with small but stable spontaneous polarization of approximately 1–5 $\mu C\ cm^{-2}$
Understanding the scaling limits, controlling and exploiting dynamics: magnetoelectric coupling at $<$20 nm length scale; $<$1 nsec time scale; $<$100 kT energy scale	Integration and scale-up of synthetic approaches to enable manufacturing would be valuable
From a longer timescale perspective, reaching the theoretical Landauer limit for switching (kT(ln2) would be desirable and will require significant effort	Convergence of memory and logic

peripheral electronics, are key challenges. An oxide-based ferromagnet or ferrimagnet that couples strongly to $BiFeO_3$ and has a Curie temperature well above room temperature would be desirable.

The recent discovery of polar vortices and skyrmions in ferroelectric superlattices presents a tantalizing opportunity to create analogous, coupled spin–charge textures out of multiferroics such as BFO [96–99]. This could present a unique pathway to overcome the antiferromagnetic ground state through such curling patterns spin/dipolar patterns. A first set of studies has been carried out to explore the possibility of forming polar textures in the BFO system [92]. Imposing electrostatic boundary conditions by interfacing to a lattice-matched, non-polar La-BFO, however, leads to the formation of an array of 109° domains as well as stabilizing an anti-polar structure in the BFO layer [95]. These results seem to suggest that while the idea of imposing electrostatic boundary conditions does work in a general sense, the consequences are governed more by the structural details, particularly the octahedral tilts that are such a key component of the crystal structure of BFO. The rather surprising outcome of the formation of the anti-polar structure can be rationalized through the fact that the electrostatic energy is more than sufficient to raise the free energy of the polar phase above that of the anti-polar phase [95]. Indeed, this seems to be a hallmark of the BFO system, where a number of phases are within a close proximity in energy scale to the ground state [100].

It is noteworthy that, although the focus of this article is on the materials physics aspects, crystal chemistry plays a dominant role in establishing the ground state of the material as well as the long-term degradation. A good example of this is the role of oxygen vacancies in inducing polarization fatigue in ferroelectrics. Such charged defects can play an equally important role in defining the degradation behaviour of multiferroics. The role of defects (point defects, dislocations and interfaces) is only going to become even more important as we get into the

sub-10 nm thickness regime. At this scale, we need to be able to account for each atom in the film as well as the cationic perfection of the structure. Indeed, this could be said for the field of complex oxides. Unlike Si-based electronics, where, until recently, the materials have been relatively simple, in the case of oxides complexity is an inherent feature.

Another aspect that would benefit from a detailed crystal chemistry-based phase equilibrium study is the formation of metastable phases; for example, one could be looking for polytypoids (phases that have the same crystal structure but a different chemical/stacking sequence, for example, Y–Si–Al–O–N's) [101] of the $BiFeO_3$ composition or chemically distinct derivatives thereof. Two examples of this could be: (i) based on the hexagonal BaM-type layered ferrites [102], (ii) the Ruddelsen–Popper-type perovskites or the Aurivillius-type phases [103]. Of these, multiferroic behaviour has been demonstrated in the hexagonal ferrites [33]. Further, chemically substituted Aurivillius phases have been known to exhibit magnetoelectric behaviour, although the magnetic state is not a robust ground state (more like a spin glass) [84]. On this note, it seems worthwhile to start with ferrimagnets (such as the layered hexaferrites) and attempt to induce a robust ferroelectric state into them, through chemical substitution or epitaxy [104]. Charge-ordering transitions, such as the Verwey transition in Fe_3O_4, were thought to lead to breaking inversion symmetry [105]; demonstrating a robust magnetoelectric effect in such systems as well as the others described in this section should be a focus for research in the coming years.

In terms of the magnetoelectric nanocomposites [63,106], several opportunities for future research are available. One would be to explore pathways by which the interface between the ferrimagnetic nanopillar is exchange-coupled to the matrix phase (for example, bismuth ferrite). Work so far has demonstrated that there is strong enhancement in the magnetic anisotropy of the magnetic phase (mediated through a three-dimensional heteroepitaxy at the nanopillar–matrix interface); creating such an exchange bias will require the existence of pinned uncompensated spins at that interface. If this can be accomplished, perhaps through improving the structural and chemical perfection of this interface, then the possibility of using just an electric field to manipulate this interfacial coupling to reverse the magnetization direction (without the application of any magnetic field) in the ferrimagnetic nanopillar exists. This would be a growth challenge because the spinel and perovskite phases are typically lattice mismatched by approximately 5%. From the synthesis perspective, it is noteworthy that the crystal chemistry aspects of such nanocomposites and the long-range order among the nanopillars is still an open question. So also, what are the limits of the lateral dimensions of the nanopillars? Another pathway to achieve magnetoelectric coupling that is yet to be explored is to use a spinel-perovskite magnetic nanocomposite (such as LSMO-$NiFe_2O_4$) that is magnetically coupled to a multiferroic such as BFO across the lateral interface (like that described in figure 12). This could be a pathway to enhance the exchange coupling temperature to room temperature (compared with the 100 K for the LSMO/BFO interface, figure 13). Such a three-level nanocomposite has recently been demonstrated with strong electric field manipulation of the exchange coupling at room temperature. This appears to be a very fruitful direction to pursue [107].

A topic that would be of significant interest is multiferroic and magnetoelectric behaviour in non-oxide materials. This has not been explored extensively as yet, although some of the early multiferroics were fluorides [108]. There are examples of magnetic nitrides (e.g. Fe_4N) [109] and nitride-based piezoelectrics and ferroelectrics are emerging [110–113]. There are fewer experimental studies of the ferroelectric polarization and its switchability, which would be a key requirement for applications. Doping or alloying the ferroelectric nitrides to induce magnetic order could be one pathway. An easier pathway may be to use heterostructuring to induce coupling. Of course, if this coupling is primarily strain-based, then manipulating the magnetization direction with an electric field will be difficult; instead, one may have to use this to manipulate the anisotropy of the magnet.

What are the limits on the length scales of the spin–charge coupling? For example, can we manipulate the spin state of a single ion using an electric field? Recent work in this

direction is poised to impact not only the fundamental physics of spin–orbit coupling and its coherent manipulation with an electric field, but also has the potential to impact the field of quantum computing, in which all of the coherent operations are carried out using an electric field [114]. Although impurities in ferroelectrics is a well-studied subject, including probing them with electron paramagnetic resonance [115], there has been very little focus on coherent manipulation of the electron spins in such systems. Recent work has shown that this is indeed possible. Ab initio calculations show that the spins in tetragonal lead titanate are aligned in a plane perpendicular to the spontaneous polarization direction, as a direct consequence of the magnetocrystalline anisotropy from spin–orbit coupling. When the spontaneous polarization is rotated by the application of an electric field, the spin easy plane also rotates by the same angle. Furthermore, electric field-controlled Hahn spin echo studies have shown that the EPR spin echo can be manipulated by an electric field, thus presenting the possibility of an all-electric field manipulation of spins.

We expect dynamical effects in multiferroics to increase in importance over the next years, driven by new experimental capabilities such as ultra-fast X-ray sources [116],[1] and that the fundamental limits on the dynamics of spin–charge–lattice coupling phenomena will be experimentally established. Theoretical proposals of dynamical multiferroic phenomena, in which a time-dependent polarization induces a magnetization in the reciprocal manner from that in which spin spirals induce polarization [117], should be validated by careful experiments. At the same time, more work on antiferromagnetic resonance in multiferroics is required; while many studies were carried out in the 1960s [118] and 1970s on conventional antiferromagnets, such measurements with modern multiferroics, which typically have higher resonance frequencies (approx. 700 GHz in $BiFeO_3$ [119], compared with approx. 350 GHz in perovskite orthoferrites [118]), have been scarce. The recent surge in antiferromagnetic spintronics should be a welcome boost to such studies [120]. On top of the materials physics/chemistry issues outlined above, there is significant potential for translational research in this field. As discussed by Manipatruni *et al*., applications such as the MESO, logic-in-memory device will require integration with Si peripheral circuitry. While this was perceived to be a challenge 20 years ago, the process integration issues have all been well addressed in the process of integrating other oxide ferroelectrics (such as lead zirconate titanate and, more recently, the hafnium zirconate tantalate ferroelectrics). But it is also clear to us that one should get into the process integration after the key fundamental issues are sorted out.

It is clear that the field of multiferroics and magnetoelectrics is poised to make further significant breakthroughs and we hope that this article motivates additional research on this fascinating class of materials and their applications. While scientific interest in the field is beyond question, the need to identify market niches and enable pathways to products, so that multiferroics go beyond being an 'area to watch' and address contemporary technological challenges. To achieve this, a shift of focus from fundamental materials discoveries to translational research and development will be needed, similar to that which occurred in the field of GaN-based light-emitting diodes two decades ago. The complexity of oxide-based material systems raises particular additional challenges, as we have seen, for example, in the colossal magnetoresistive manganites, making the active engagement of applied physicists and device engineers early in the research and development process even more essential. In this vein, the recent engagement of large microelectronic companies in the field of multiferroics [101,102] is particularly encouraging. While basic research in multiferroics is vibrant, the field would benefit from an injection of focused programmes that address the transition to devices, in particular scale-up and integration issues.

Data accessibility. This article has no additional data.
Authors' contributions. S.M. and R.R. co-wrote the review.
Competing interests. We declare we have no competing interests.
Funding. We received no funding for this study.

[1]For example, Linac Coherent Light Source (LCLS) at Stanford Linear Accelerator Center, Stanford University.

Acknowledgements. We have written this article on behalf of many collaborators, co-workers, students and postdocs worldwide and acknowledge their intellectual participation and contribution. The rapid pace of development in this field means that it is impossible to acknowledge and cite each of them independently. We encourage the interested reader to look at the review articles cited in this paper as well as to reach out to us if we can be of further assistance. Our work, especially in the academic world, would not have been possible without the sustained support of federal and industrial funding agencies. Particularly, the sustained support of the U.S. Department of Energy Basic Energy Sciences Office, the Semiconductor Research Corporation's JUMP Initiative, the National Science Foundation, specifically the MRSEC program, the Army Research Office, and Intel Corp., is gratefully acknowledged.

References

1. Manipatruni S, Nikonov DE, Young IA. 2018 Beyond CMOS computing with spin and polarization. *Nat. Phys.* **14**, 338–343. (doi:10.1038/s41567-018-0101-4)
2. Khan HN, Hounshell DA, Fuchs ERH. 2018 Science and research policy at the end of Moore's law. *Nat. Electron.* **1**, 14–21. (doi:10.1038/s41928-017-0005-9)
3. Wikipedia.
4. Moore GE. 1998 Cramming more components onto integrated circuits. *Proc. IEEE* **86**, 82–85. (doi:10.1109/JPROC.1998.658762)
5. Dennard RH, Rideout VL, Bassous E, Leblanc AR. 1974 Design of ion-implanted MOSFET's with very small physical dimensions. *IEEE J. Solid-State Circuits* **9**, 256–268. (doi:10.1109/JSSC.1974.1050511)
6. Shannon CE. 1971 A Universal Turing machine with two internal states. *J. Symb. Log.* **36**, 532.
7. Kuhn KJ. 2012 Considerations for ultimate CMOS scaling. *IEEE Trans. Electron Devices* **59**, 1813–1828. (doi:10.1109/TED.2012.2193129)
8. Ferain I, Colinge CA, Colinge J-P. 2011 Multigate transistors as the future of classical metal-oxide-semiconductor field-effect transistors. *Nature* **479**, 310–316. (doi:10.1038/nature10676)
9. Theis TN, Solomon PM. 2010 It's time to reinvent the transistor! *Science* **327**, 1600–1601. (doi:10.1126/science.1187597)
10. Manipatruni S *et al.* 2019 Magnetoelectric spin orbit logic: a scalable charge mediated nonvolatile logic. *Nature* **565**, 35–42. (doi:10.1038/s41586-018-0770-2)
11. Salahuddin S, Datta S. 2018 The era of hyperscaling in electronics. *Nat. Electron.* **442**, 442–450. (doi:10.1038/s41928-018-0117-x)
12. Patterson DA, Hennessy JL. 2017 *Computer architecture: a quantitative approach*, 6th edn. The Morgan Kaufman Series. Amsterdam, The Netherlands: Elsevier.
13. Borders WA, Pervaiz AZ, Fukami S, Camsari KY, Ohno H, Datta S. 2019 Integer factorization using stochastic magnetic tunnel junctions. *Nature* **573**, 390–393. (doi:10.1038/s41586-019-1557-9)
14. Technical Report 2009 Adapted from Gadgets and Gigawatts, Policies for Energy Efficient Electronics, International Energy Agency.
15. Jin S, Tiefel TH, McCormack M, Fastnacht RA, Ramesh R, Chen LH. 1994 Thousandfold change in resistivity in magnetoresistive La-Ca-Mn-O films. *Science* **264**, 413–415. (doi:10.1126/science.264.5157.413)
16. Imada M, Fujimori A, Tokura Y. 1998 Metal-insulator transitions. *Rev. Mod. Phys.* **70**, 1039–1262. (doi:10.1103/RevModPhys.70.1039)
17. Chikazumi S. 1964 *Physics of magnetism*. New York, NY: Wiley Publishers.
18. Dieny B *et al.* 2020 Opportunities and challenges for spintronics in the microelectronics industry. *Nat. Electron.* **446**, 446–459. (doi:10.1038/s41928-020-0461-5)
19. Wu T, Ogale SB, Garrison JE, Nagaraj B, Biswas A, Chen Z, Greene RL, Ramesh R, Venkatesan T. 2001 Electroresistance and electronic phase separation in mixed-valent manganites. *Phys. Rev. Lett.* **86**, 5998–6001. (doi:10.1103/PhysRevLett.86.5998)
20. Song C, Cui B, Li F, Zhou X, Pan F. 2017 Recent progress in voltage control of magnetism: materials, mechanisms, and performance. *Prog. Mater Sci.* **87**, 33–82. (doi:10.1016/j.pmatsci.2017.02.002)
21. Spaldin NA, Ramesh R. 2019 Advances in magnetoelectric multiferroics. *Nat. Mater.* **18**, 203–212. (doi:10.1038/s41563-018-0275-2)
22. Schmid H. 1994 Multiferroic magnetoelectrics. *Ferroelectrics* **162**, 317. (doi:10.1080/00150199408245120)

23. Fiebig M. 2005 Revival of the magnetoelectric effect. *J. Phys. D* **38**, R123. (doi:10.1088/0022-3727/38/8/R01)
24. Ramesh R, Spaldin NA. 2007 Multiferroics: progress and prospects in thin films. *Nature Mater.* **6**, 203–212. (doi:10.1038/nmat1805)
25. Science (eds) 2007 Areas to watch. *Science* **318**, 1848–1849. (doi:10.1126/science.318.5858.1848)
26. Ullakko K. 1996 Magnetically controlled shape memory alloys: a new class of actuator materials. *J. Mater. Eng. Perform.* **5**, 405–409. (doi:10.1007/BF02649344)
27. Hill NA. 2000 Why are there so few magnetic ferroelectrics? *J. Phys. Chem. B* **104**, 6694. (doi:10.1021/jp000114x)
28. Wang Y, Hu J, Lin Y, Nan C-W. 2010 Multiferroic magnetoelectric composite nanostructures. *NPG Asia Mater.* **2**, 61–68.
29. Pyatakov AP, Zvezdin AK. 2012 Magnetoelectric and multiferroic media. *Phys. – Uspekhi* **55**, 557. (doi:10.3367/UFNe.0182.201206b.0593)
30. Tokura Y, Seki S, Nagaosa N. 2014 Multiferroics of spin origin. *Rep. Prog. Phys.* **77**, 076501. (doi:10.1088/0034-4885/77/7/076501)
31. Dong S, Liu J-M, Cheong SW, Ren Z. 2015 Multiferroic materials and magnetoelectric physics: symmetry, entanglement, excitation, and topology. *Adv. Phys.* **64**, 519–626. (doi:10.1080/00018732.2015.1114338)
32. Fiebig M, Lottermoser T, Meier D, Trassin M. 2016 The evolution of multiferroics. *Nat. Rev. Mater.* **1**, 16046. (doi:10.1038/natrevmats.2016.46)
33. Kimura T, Goto T, Shintani H, Ishizaka K, Arima T, Tokura Y. 2003 Magnetic control of ferroelectric polarization. *Nature* **426**, 55–58. (doi:10.1038/nature02018)
34. Mundy J *et al.* 2016 Atomically engineered ferroic layers yield a room temperature magnetoelectric multiferroic. *Nature* **537**, 523–527. (doi:10.1038/nature19343)
35. Wang J *et al.* 2003 Epitaxial $BiFeO_3$ multiferroic thin film heterostructures. *Science* **299**, 1719–1722. (doi:10.1126/science.1080615)
36. Catalan G, Scott JF. 2009 Physics and applications of bismuth ferrite. *Adv. Mater.* **21**, 2463–2485. (doi:10.1002/adma.200802849)
37. Neaton JB, Ederer C, Waghmare UV, Spaldin NA, Rabe KM. 2005 First-principles study of spontaneous polarization in multiferroic $BiFeO_3$. *Phys. Rev. B* **71**, 014113. (doi:10.1103/PhysRevB.71.014113)
38. Zvezdin AK, Kadomtseva AM, Krotov SS, Pyatakov AP, Popov YF, Vorob'Ev GP. 2006 Magnetoelectric interaction and magnetic field control of electric polarization in multiferroics. *J. Magn. Magn. Mater.* **300**, 224–228. (doi:10.1016/j.jmmm.2005.10.068)
39. Martin LW, Chu YH, Holcomb MB, Huijben M, Han SJ, Lee D, Wang SX, Ramesh R. 2008 Nanoscale control of exchange bias with $BiFeO_3$ thin films. *Nanoletters* **8**, 2050–2055.
40. He Q *et al.* 2012 Magnetotransport at domain walls in $BiFeO_3$. *Phys. Rev. Lett.* **108**, 067203. (doi:10.1103/PhysRevLett.108.067203)
41. Yang CH, Kan D, Takeuchi I, Nagarajan V, Seidel J. 2012 Doping $BiFeO_3$: approaches and enhanced functionality. *Phys. Chem. Chem. Phys.* **14**, 15 953–15 962. (doi:10.1039/c2cp43082g)
42. Kan D, Pálová L, Anbusathaiah V, Cheng CJ, Fujino S, Nagarajan V, Rabe KM, Takeuchi I. 2010 Universal behavior and electric-field-induced structural transition in rare-earth-substituted $BiFeO_3$. *Adv. Funct. Mater.* **20**, 1108–1115. (doi:10.1002/adfm.200902017)
43. Huang Y *et al.* 2020 Manipulating magnetoelectric energy landscape in multiferroics. *Nat. Commun.* **11**, 1–8. (doi:10.1038/s41467-020-16727-2)
44. Naganuma H, Yasui S, Nishida K, Iijima T, Funakubo H, Okamura S. 2011 Enhancement of magnetization at morphotropic phase boundary in epitaxial $BiCoO_3$-$BiFeO_3$ solid solution films grown on $SrTiO_3$ (100) substrates. *J. Appl. Phys.* **109**, 07D917. (doi:10.1063/1.3561776)
45. Yasui S, Nishida K, Naganuma H, Okamura S, Iijima T, Funakubo H. 2007 Crystal structure analysis of epitaxial $BiFeO_3$–$BiCoO_3$ solid solution films grown by metalorganic chemical vapor deposition. *Japanese J. Appl. Phys.* **46**, 6948–6951. (doi:10.1143/JJAP.46.6948)
46. Yasui S, Sakata O, Nakajima M, Utsugi S, Yazawa K, Yamada T, Funakubo H. 2009 Piezoelectric properties of {100}-oriented epitaxial $BiCoO_3$–$BiFeO_3$ films measured using synchrotron X-ray diffraction. *Japan. J. Appl. Phys.* **48**, 09KD06.
47. Singha MK, Yanga Y, Christos G. 2009 Takoudis. *Coord. Chem. Rev.* **253**, 2920–2934. (doi:10.1016/j.ccr.2009.09.003)
48. Maksymovych P *et al.* 2012 Ultrathin limit and dead-layer effects in local polarization switching of $BiFeO_3$. *Phys. Rev. B* **85**, 014119. (doi:10.1103/PhysRevB.85.014119)

49. Zhong W, Vanderbilt D, Rabe KM. 1994 Phase transitions in $BaTiO_3$ from first principles. *Phys. Rev. Lett.* **73**, 1861–1864. (doi:10.1103/PhysRevLett.73.1861)
50. Rabe KM, Waghmare UV. 1995 Localized basis for effective lattice Hamiltonians: Lattice Wannier functions. *Phys. Rev. B* **52**, 13236. (doi:10.1103/PhysRevB.52.13236)
51. Liu S, Grinberg I, Rappe AM. 2013 Development of a bond-valence based interatomic potential for $BiFeO_3$ for accurate molecular dynamics simulations. *J. Phys. Condens. Matter* **25**, 102202. (doi:10.1088/0953-8984/25/10/102202)
52. Rahmedov D, Wang D, Íñiguez J, Bellaiche L. 2012 Magnetic cycloid of $BiFeO_3$ from atomistic simulations. *Phys. Rev. Lett.* **109**, 037207. (doi:10.1103/PhysRevLett.109.037207)
53. Karpinsky DV *et al.* 2017 Thermodynamic potential and phase diagram for multiferroic bismuth ferrite ($BiFeO_3$). *NPJ Comp. Mater.* **3**, 20. (doi:10.1038/s41524-017-0021-3)
54. Garcia-Fernandez P, Wojdel JC, Iniguez J, Junquera J. 2016 Second-principles method for materials simulations including electron and lattice degrees of freedom. *Phys. Rev. B* **93**, 195137. (doi:10.1103/PhysRevB.93.195137)
55. Wojdel JC, Hermet P, Ljungberg MP, Ghosez P, Iniguez J. 2013 First-principles model potentials for lattice-dynamical studies: general methodology and example of application to ferroic perovskite oxides. *J. Phys.: Condens. Matter* **25**, 305401. (doi:10.1088/0953-8984/25/30/305401)
56. Liu S, Grinberg I, Rappe AM. 2016 Intrinsic ferroelectric switching from first principles. *Nature* **534**, 360–363. (doi:10.1038/nature18286)
57. Bhattacharjee S, Rahmedov D, Wang D, Íñiguez J, Bellaiche L. 2014 Ultrafast switching of the electric polarization and magnetic chirality in $BiFeO_3$ by an electric field. *Phys. Rev. Lett.* **112**, 147601. (doi:10.1103/PhysRevLett.112.147601)
58. Wang D, Weerasinghe J, Albarakati A, Bellaiche L. 2013 Terahertz dielectric response and coupled dynamics of ferroelectrics and multiferroics from effective Hamiltonian simulations. *Int. J. Mod. Phys. B* **27**, 1330016. (doi:10.1142/S0217979213300168)
59. Rana DS, Kawayama I, Mavani K, Takahashi K, Murakami H, Tonouchi M. 2009 Understanding the nature of ultrafast polarization dynamics of ferroelectric memory in the multiferroic $BiFeO_3$. *Adv. Mater.* **21**, 2881–2885. (doi:10.1002/adma.200802094)
60. Spaldin NA, Fiebig M, Mostovoy M. 2008 The toroidal moment in condensed-matter physics and its relation to the magnetoelectric effect. *J. Phys.: Condens. Matter* **20**, 434203. (doi:10.1088/0953-8984/20/43/434203)
61. Tolédano P, Ackermann M, Bohaty L, Becker P, Lorenz T, Leo N, Fiebig M. 2015 Primary ferrotoroidicity in antiferromagnets. *Phys. Rev. B* **92**, 094431. (doi:10.1103/PhysRevB.92.094431)
62. Zhao T *et al.* 2006 Electrical control of antiferromagnetic domains in multiferroic $BiFeO_3$ films at room temperature. *Nat. Mater.* **5**, 823–829. (doi:10.1038/nmat1731)
63. Lebeugle D, Colson D, Forget A, Viret M, Bataille AM, Gukasov A. 2008 Electric-field-induced spin flop in $BiFeO_3$ single crystals at room temperature. *Phys. Rev. Lett.* **100**, 227602. (doi:10.1103/PhysRevLett.100.227602)
64. Zheng H *et al.* 2004 Multiferroic $BaTiO_3$-$CoFe_2O_4$ nanostructures. *Science* **303**, 661–663. (doi:10.1126/science.1094207)
65. Zavaliche F *et al.* 2005 Electric field-induced magnetization switching in epitaxial columnar nanostructures. *Nano Lett.* **5**, 1793–1796. (doi:10.1021/nl051406i)
66. He X *et al.* 2010 Robust isothermal electric control of exchange bias at room temperature. *Nat. Mater.* **9**, 579–585. (doi:10.1038/nmat2785)
67. Cherifi RO *et al.* 2014 Electric-field control of magnetic order above room temperature. *Nat. Mater.* **13**, 345–351. (doi:10.1038/nmat3870)
68. Gruner M, Hoffmann E, Entel P. 2003 Instability of the rhodium magnetic moment as the origin of the metamagnetic phase transition in α-FeRh. *Phys. Rev. B* **67**, 064415. (doi:10.1103/PhysRevB.67.064415)
69. Moruzzi VL, Marcus PM. 1992 Antiferromagnetic-ferromagnetic transition in FeRh. *Phys. Rev. B* **46**, 2864–2873. (doi:10.1103/PhysRevB.46.2864)
70. Lee Y *et al.* 2015 Large resistivity modulation in mixed-phase metallic systems. *Nat. Commun.* **6**, 5959. (doi:10.1038/ncomms6959)
71. Allibe J, Fusil S, Bouzehouane K, Daumont C, Sando D, Jacquet E, Deranlot C, Bibes M, Barthelemy A. 2012 Room temperature electrical manipulation of giant magnetoresistance in spin valves exchange-biased with $BiFeO_3$. *Nano Lett.* **12**, 1141–1145. (doi:10.1021/nl202537y)

72. Heron JT *et al.* 2014 Deterministic switching of ferromagnetism at room temperature using an electric field. *Nature* **516**, 370–373. (doi:10.1038/nature14004)
73. Wu SM, Cybart SA, Yu P, Rossell MD, Zhang JX, Ramesh R, Dynes RC. 2010 Reversible electric control of exchange bias in a multiferroic field effect device. *Nat. Mater.* **9**, 756–761. (doi:10.1038/nmat2803)
74. Yu P *et al.* 2012 Interface control of bulk ferroelectric polarization. *Proc. Natl Acad. Sci. USA* **109**, 9710–9715. (doi:10.1073/pnas.1117990109)
75. Suzuki Y. 2001 Epitaxial spinel ferrite thin films. *Annu. Rev. Mater. Res.* **31**, 265–289. (doi:10.1146/annurev.matsci.31.1.265)
76. Serrate D, De Teresa JM, Ibarra MR. 2007 Double perovskites with ferromagnetism above room temperature. *J. Phys.: Condens. Matter* **19**, 023201. (doi:10.1088/0953-8984/19/2/023201)
77. Liu ZQ *et al.* 2016 Full electroresistance modulation in a mixed-phase metallic alloy. *Phys. Rev. Lett.* **116**, 097203. (doi:10.1103/PhysRevLett.116.097203)
78. Yi D, Liu J, Okamoto S, Jagannatha S, Chen YC, Yu P, Chu YH, Arenholz E, Ramesh R. 2013 Tuning the competition between ferromagnetism and antiferromagnetism in a half-doped manganite through magnetoelectric coupling. *Phys. Rev. Lett.* **111**, 127601. (doi:10.1103/PhysRevLett.111.127601)
79. Heron JT, Schlom DG, Ramesh R. 2014 Electric field control of magnetism using $BiFeO_3$-based heterostructures. *Appl. Phys. Rev.* **1,** 021303. (doi:10.1063/1.4870957)
80. Prasad B *et al.* 2020 Ultralow voltage manipulation of ferromagnetism. *Adv. Mater.* **32**, 2001943. (doi:10.1002/adma.202001943)
81. Zutic I, Fabian J, Das Sarma S. 2004 Spintronics: fundamentals and applications. *Rev. Modern Phys.* **76**, 323. (doi:10.1103/RevModPhys.76.323)
82. Nakayama H, Kanno Y, An H, Tashiro T, Haku S, Nomura A, Ando K. 2016 Rashba-Edelstein magnetoresistance in metallic heterostructures. *Phys. Rev. Lett.* **117**, 116602. (doi:10.1103/PhysRevLett.117.116602)
83. Hoffmann A, Bader SD. 2015 Opportunities at the frontiers of spintronics. *Phys. Rev. Appl.* **4**, 047001. (doi:10.1103/PhysRevApplied.4.047001)
84. Smolenskii GA, Chupis IE. 1982 Ferroelectromagnets. *Usp. Fiz. Nauk* **137**, 415–448. (doi:10.3367/UFNr.0137.198207b.0415)
85. Li J, Nagaraj B, Liang H, Cao W, Lee CH, Ramesh R. 2004 Ultrafast polarization switching in thin-film ferroelectrics. *Appl. Phys. Lett.* **84**, 1174–1176. (doi:10.1063/1.1644917)
86. Parsonnet E *et al.* 2020 Toward intrinsic ferroelectric switching in multiferroic $BiFeO_3$. *Phys. Rev. Lett.* **125**, 067601. (doi:10.1103/PhysRevLett.125.067601)
87. Rabe KM, Ahn CH, Triscone J-M. 2007 *Physics of ferroelectrics, A modern perspective*. Springer Topics in Applied Physics. Berlin, Germany: Springer.
88. Steffes JJ, Ristau RA, Ramesh R, Huey BD. 2019 Thickness scaling of ferroelectricity in $BiFeO_3$ by tomographic atomic force microscopy. *Proc. Natl Acad. Sci.* **116**, 2413–2418. (doi:10.1073/pnas.1806074116)
89. Chandra P, Dawber M, Littlewood PB, Scott JF. 2004 Scaling of the coercive field with thickness in thin-film ferroelectrics. *Ferroelectrics* **313**, 7–13. (doi:10.1080/00150190490891157)
90. Chu YH *et al.* 2008 Low voltage performance of epitaxial $BiFeO_3$ films on Si substrates through lanthanum substitution. *Appl. Phys. Lett.* **92**, 102909. (doi:10.1063/1.2897304)
91. Lesne E *et al.* 2016 Highly efficient and tunable spin-to-charge conversion through Rashba coupling at oxide interfaces. *Nat. Mater.* **15**, 1261–1266. (doi:10.1038/nmat4726)
92. Batra IP, Wurfel P, Silverman BD. 1973 Phase transition, stability, and depolarization field in ferroelectric thin films. *Phys. Rev. B* **8**, 3257–3265. (doi:10.1103/PhysRevB.8.3257)
93. Jain A *et al.* 2018 The materials project: accelerating materials design through theory-driven data and tools. In *Handbook of materials modeling* (eds W Andreoni, S Yip). Berlin, Germany: Springer.
94. Ramesh R, Schlom DG. 2019 Creating emergent phenomena in oxide superlattices. *Nat. Rev. Mater.* **4,** 257–268. (doi:10.1038/s41578-019-0095-2)
95. Fan S *et al.* 2020 Site-specific spectroscopic measurement of spin and charge in $(LuFeO_3)m/(LuFe_2O_4)1$ multiferroic superlattices. *Nat. Commun.* **11**, 1–9. (doi:10.1038/s41467-020-19285-9)
96. Yadav AK *et al.* 2016 Observation of polar vortices in oxide superlattices. *Nature* **530**, 198–201. (doi:10.1038/nature16463)

97. Das S *et al.* 2019 Observation of room temperature polar skyrmions. *Nature* **568**, 368–372. (doi:10.1038/s41586-019-1092-8)
98. Das S *et al.* 2020 Local negative permittivity and topological phase transition in polar skyrmions. *Nat. Mater.* **20**, 194–201. (doi:10.1038/s41563-020-00818-y)
99. Mundy J *et al.* 2021 Liberating a hidden antiferroelectric phase with interfacial electrostatic engineering. *Sci. Adv.* submitted.
100. Diéguez O, González-Vázquez OE, Wojdeł JC, Íñiguez J. 2011 First-principles predictions of low-energy phases of multiferroic $BiFeO_3$. *Phys. Rev. B* **83**, 094105. (doi:10.1103/PhysRevB.83.094105)
101. Thompson DP, Korgul P, Hendry A. 1983 The structural characterisation of Si-Al-O-N polytypoids. In *Progress in nitrogen ceramics. NATO ASI series (series E: applied sciences)*, vol 65 (ed, FL Riley), Dordrecht, The Netherlands: Springer.
102. Kimura T. 2012 Magnetoelectric hexaferrites. *Annu. Rev. Condens. Matter Phys.* **3**, 93–110. (doi:10.1146/annurev-conmatphys-020911-125101)
103. Lee D, Lee HN. 2017 Controlling oxygen mobility in ruddlesden–popper oxides. *Materials* **10**, 368. (doi:10.3390/ma10040368)
104. Chen T *et al.* 2021 A new room temperature multiferroic bismuth hexaferrite. *Nature.* submitted.
105. Ikeda N *et al.* 2005 Ferroelectricity from iron valence ordering in the charge-frustrated system $LuFe_2O_4$. *Nature* **436**, 1136–1138. (doi:10.1038/nature04039)
106. Zhang W, Chen A, Bi Z, Jia Q, MacManus-Driscoll JL, Wang H. 2014 Interfacial coupling in heteroepitaxial vertically aligned nanocomposite thin films: from lateral to vertical control. *Curr. Opin. Solid State Mater. Sci.* **18**, 6–18. (doi:10.1016/j.cossms.2013.07.007)
107. Wu R *et al.* 2021 Self-biased magnetoelectric switching at room temperature in three phase ferroelectric-antiferroelectric-ferrimagnetic nanocomposites. *Nat. Electron.* **4**, 333–341. (doi:10.1038/s41928-021-00584-y)
108. Scott JF, Blinc R. 2011 Multiferroic magnetoelectric fluorides: why are there so many magnetic ferroelectrics? *J. Phys.: Condens. Matter.* **23**, 113202. (doi:10.1088/0953-8984/23/11/113202)
109. Coey JMD, Smith PAI. 1999 Magnetic nitrides. *J. Magn. Magn. Mater.* **200**, 405–424. (doi:10.1016/S0304-8853(99)00429-1)
110. Jena D *et al.* 2019 The new nitrides: layered, ferroelectric, magnetic, metallic and superconducting nitrides to boost the GaN photonics and electronics eco-system. *Japan. J. Appl. Phys.* **58**, SC0801. (doi:10.7567/1347-4065/ab147b)
111. Talley KR, Perkins CL, Diercks DR, Brennecka GL, Zakutayev A. 2001 Synthesis of ferroelectric LaWN3 - the first nitride perovskite. (http://arxiv.org/abs/2001.00633).
112. Sarmiento-Pérez R, Cerqueira TF, Körbel S, Botti S, Marques MA. 2015 Prediction of stable nitride perovskites. *Chem. Mater.* **27**, 5957–5963. (doi:10.1021/acs.chemmater.5b02026)
113. Zhang S, Holec D, Fu WY, Humphreys CJ, Moram MA. 2013 Tunable optoelectronic and ferroelectric properties in Sc-based III-nitrides. *J. Appl. Phys.* **114**, 133510. (doi:10.1063/1.4824179)
114. Liu J *et al.* 2021 Coherent electric field manipulation of Fe^{+3}-spins in $PbTiO_3$. *Sci. Adv.* **7**, eabf81033.
115. Mïüller KA. 1981 Paramagnetic point and pair defects in oxide perovskites. *J. Physique* **42**, 551–557. (doi:10.1051/jphys:01981004204055100)
116. Dhillon SS *et al.* 2017 The 2017 terahertz science and technology road map. *J. Phys D: Appl. Phys.* **50**, 043001. (doi:10.1088/1361-6463/50/4/043001)
117. Juraschek D, Fechner M, Balatsky AV, Spaldin NA. 2017 Dynamical multiferroicity. *Phys. Rev. Mater.* **1**, 104401.
118. Abraha K, Tilley DR. 1996 Theory of far infrared properties of magnetic surfaces, films and superlattices. *Surf. Sci. Rep.* **24**, 129–222. (doi:10.1016/0167-5729(96)00003-9)
119. Talbayev D, Trugman SA, Lee S, Yi HT, Cheong SW, Taylor AJ. 2011 Long-wavelength magnetic and magnetoelectric excitations in the ferroelectric antiferromagnet $BiFeO_3$. *Phys. Rev. B* **83**, 094403. (doi:10.1103/PhysRevB.83.094403)
120. Jungwirth T, Marti X, Wadley P, Wunderlich J. 2016 Antiferromagnetic spintronics. *Nat. Nanotechnol.* **11**, 231–341. (doi:10.1038/nnano.2016.18)